

1   **An antisense RNA capable of modulating the  
2   expression of the tumor suppressor microRNA-34a**  
3

4   **Jason T. Serviss<sup>1\*</sup>, Felix Clemens Richter<sup>1,2</sup>, Nathanael Johansson  
5   Andrews<sup>1</sup>, Miranda Houtman, Laura Schwarzmüller, Per Johnsson,  
6   Jimmy Van Den Eynden, Erik Larsson<sup>3</sup>, Dan Grandér<sup>1</sup>, Katja Pokrovskaia  
7   Tamm<sup>1</sup>**

8  
9   <sup>1</sup> Department of Oncology and Pathology, Karolinska Institutet, Stockholm,  
10   Sweden

11   <sup>2</sup> Kennedy Institute of Rheumatology, University of Oxford, Roosevelt Drive,  
12   Oxford OX3 7FY, UK

13   <sup>3</sup>Department of Medical Biochemistry and Cell Biology, Institute of  
14   Biomedicine, The Sahlgrenska Academy, University of Gothenburg, SE-405  
15   30 Gothenburg, Sweden

16   **\* Correspondence:**

17   Jason T. Serviss, Department of Oncology and Pathology, Karolinska  
18   Institutet, Stockholm, Sweden, SE-17177. [jason.serviss@ki.se](mailto:jason.serviss@ki.se)

21   **Abstract**

23   The microRNA-34a is a well-studied tumor suppressor microRNA (miRNA)  
24   that is a direct down-stream target of TP53 and has roles in multiple pathways  
25   associated with oncogenesis, such as proliferation, cellular growth, and  
26   differentiation. Due to its wide variety of targets that suppress oncogenesis, it  
27   is not surprising that miR34a expression has been shown to be dys-regulated  
28   in a wide variety of both solid tumors and hematological malignancies.  
29   Despite this, the mechanisms by which miR34a is regulated in these cancers  
30   is not well studied. Here we find that the *miR34a* antisense RNA, a long non-  
31   coding RNA transcribed antisense to *miR34a*, is critical  
32   for *miR34a* expression and mediation of its cellular functions in multiple types  
33   of human cancer. In addition, we characterize miR34a asRNA's ability to  
34   facilitate miR34a expression under multiple types of cellular stress in both  
35   TP53 deficient and wild-type settings.

36 **Introduction**

37 In recent years advances in functional genomics has revolutionized our  
38 understanding of the human genome. Evidence now points to the fact that  
39 approximately 75% of the genome is transcribed but only ~1.2% of this is  
40 responsible for encoding proteins (International Human Genome Sequencing  
41 2004, Djebali et al. 2012). Of these recently identified elements, long non-  
42 coding (lnc) RNAs are defined as transcripts exceeding 200bp in length with a  
43 lack of a functional open reading frame. Some lncRNAs are dually classified  
44 as antisense (as) RNAs that are expressed from the same locus as a sense  
45 transcript in the opposite orientation. Current estimates using high-throughput  
46 transcriptome sequencing, indicate that up to 20-40% of the approximately  
47 20,000 protein-coding genes exhibit antisense transcription (Chen et al. 2004,  
48 Katayama et al. 2005, Ozsolak et al. 2010). The hypothesis that asRNAs play  
49 an important role in oncogenesis was first proposed when studies increasingly  
50 found examples of aberrant expression of these transcripts and other lncRNA  
51 subgroups in tumor samples (Balbin et al. 2015). Although studies  
52 characterizing the functional importance of asRNAs in cancer are limited to  
53 date, characterization a number of individual transcripts has led to the  
54 discovery of multiple examples of asRNA-mediated regulation of several well  
55 known tumorigenic factors (Yap et al. 2010, Johnsson et al. 2013). The  
56 mechanisms by which asRNAs accomplish this are diverse, and include  
57 recruitment of chromatin modifying factors (Rinn et al. 2007), acting as  
58 microRNA (miRNA) sponges (Memczak et al. 2013), and causing  
59 transcriptional interference (Conley et al. 2012).

60

61 Responses to cellular stress, e.g. DNA damage, sustained oncogene  
62 expression, and nutrient deprivation, are all tightly monitored and orchestrated  
63 cellular pathways that are commonly dys-regulated in cancer. Cellular  
64 signaling in response to these types of cellular stress often converge on the  
65 transcription factor *TP53* that regulates transcription of coding and non-coding  
66 downstream targets. One non-coding target of *TP53* is the tumor suppressor  
67 microRNA known as *miR34a* (Raver-Shapira et al. 2007).  
68 Upon *TP53* activation *miR34a* expression is increased allowing it to down-  
69 regulate its targets involved in cellular pathways such as, growth factor  
70 signaling, apoptosis, differentiation, and cellular senescence (Lal et al. 2011,  
71 Slabakova et al. 2017). *miR34a* is a crucial factor in mediating activated *TP53*  
72 response and it is often deleted or down-regulated in human cancers and has  
73 also been shown to be a valuable prognostic marker (Cole et al. 2008,  
74 Gallardo et al. 2009, Zenz et al. 2009, Cheng et al. 2010, Liu et al. 2011).  
75 Reduced *miR34a* transcription is mediated via epigenetic regulation in many  
76 solid tumors, such as colorectal-, pancreatic-, and ovarian cancer (Vogt et al.  
77 2011), as well as multiple types of hematological malignancies (Chim et al.  
78 2010). In addition, *miR34a* has been shown to be transcriptionally regulated  
79 via *TP53* homologs, *TP63* and *TP73*, other transcription factors, e.g. *STAT3*  
80 and *MYC*, and, in addition, post-transcriptionally through miRNA sponging by  
81 the *NEAT1* lncRNA (Chang et al. 2008, Su et al. 2010, Agostini et al. 2011,  
82 Rokavec et al. 2015, Ding et al. 2017). Despite these findings, the  
83 mechanisms underlying *miR34a* regulation in the context of oncogenesis have  
84 not yet been fully elucidated.

85

86 Studies across multiple cancer types have reported a decrease in oncogenic  
87 phenotypes when miR34a expression is induced in a p53-null background,  
88 although endogenous mechanisms for achieving this have not yet been  
89 discovered (Liu et al. 2011, Ahn et al. 2012, Yang et al. 2012, Stahlhut et al.  
90 2015, Wang et al. 2015). In addition, previous reports have identified a  
91 lncRNA originating in the antisense orientation from the miR34a locus which  
92 is regulated by TP53 and is induced upon cellular stress (Rashi-Elkeles et al.  
93 2014, Hunten et al. 2015, Leveille et al. 2015, Ashouri et al. 2016, Kim et al.  
94 2017). Despite this, none of these studies have continued to functionally  
95 characterize this transcript. In this study we functionally characterize  
96 the *miR34a* asRNA transcript, and find that modulating the levels of  
97 the *miR34a* asRNA is sufficient to increase levels of *miR34a* and results in a  
98 decrease of multiple tumorigenic phenotypes. Furthermore, we find that  
99 miR34a asRNA-mediated up-regulation of miR34a is sufficient to induce  
100 endogenous cellular mechanisms counteracting several types of stress stimuli  
101 in a *TP53* deficient background. Finally, similar to the functional roles of  
102 antisense transcription at protein-coding genes, we find that antisense RNAs  
103 are also capable of regulating cancer-associated miRNAs.

104

## 105 **Results**

106

107 ***miR34a* asRNA is a broadly expressed, non-coding transcript whose**  
108 **levels correlate with *miR34a* expression**

109

110 *miR34a* asRNA is transcribed in a “head-to-head” orientation with  
111 approximately 100 base pair overlap with the *miR34a* host gene (HG) (**Fig.**  
112 **1a**). Due to the fact that sense/antisense pairs can be both concordantly and  
113 discordantly expressed, we sought to evaluate this relationship in the case of

114 *miR34a* HG and its asRNA. Using a diverse panel of cancer cell lines, we  
115 detected co-expression of both the *miR34a* HG and *miR34a* asRNA (**Fig. 1b**).  
116 We included *TP53*+/+, *TP53* mutated, and *TP53*-/- cell lines in the panel due  
117 to previous reports that *miR34a* is a known downstream target of TP53.  
118 These results indicate that *miR34a* HG and *miR34a* asRNA are co-expressed  
119 and that their expression levels correlate with *TP53* status, with *TP53*-/- cell  
120 lines tending to have decreased expression of both transcripts.

121

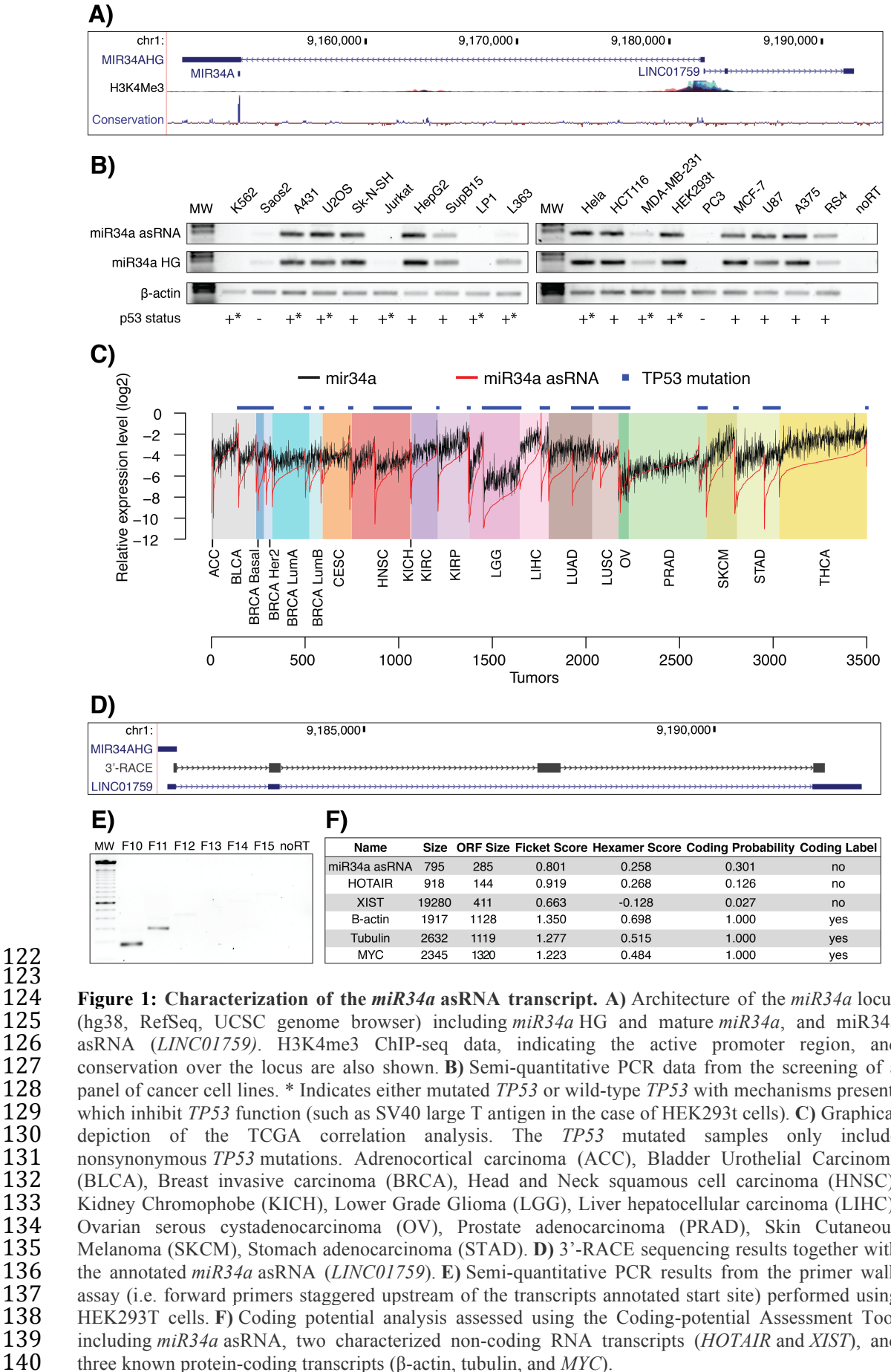


**Figure 1: Characterization of the *miR34a* asRNA transcript.** A) Architecture of the *miR34a* locus (hg38, RefSeq, UCSC genome browser) including *miR34a* HG and mature *miR34a*, and *miR34a* asRNA (*LINC01759*). H3K4me3 ChIP-seq data, indicating the active promoter region, and conservation over the locus are also shown. B) Semi-quantitative PCR data from the screening of a panel of cancer cell lines. \* Indicates either mutated *TP53* or wild-type *TP53* with mechanisms present, which inhibit *TP53* function (such as SV40 large T antigen in the case of HEK293t cells). C) Graphical depiction of the TCGA correlation analysis. The *TP53* mutated samples only include nonsynonymous *TP53* mutations. Adrenocortical carcinoma (ACC), Bladder Urothelial Carcinoma (BLCA), Breast invasive carcinoma (BRCA), Head and Neck squamous cell carcinoma (HNSC), Kidney Chromophobe (KICH), Lower Grade Glioma (LGG), Liver hepatocellular carcinoma (LIHC), Ovarian serous cystadenocarcinoma (OV), Prostate adenocarcinoma (PRAD), Skin Cutaneous Melanoma (SKCM), Stomach adenocarcinoma (STAD). D) 3'-RACE sequencing results together with the annotated *miR34a* asRNA (*LINC01759*). E) Semi-quantitative PCR results from the primer walk assay (i.e. forward primers staggered upstream of the transcripts annotated start site) performed using HEK293T cells. F) Coding potential analysis assessed using the Coding-potential Assessment Tool including *miR34a* asRNA, two characterized non-coding RNA transcripts (*HOTAIR* and *XIST*), and three known protein-coding transcripts ( $\beta$ -actin, tubulin, and *MYC*).

141 We next sought to interrogate primary cancer samples to examine if a  
142 correlation between *miR34a* asRNA and *miR34a* expression levels could be  
143 identified. For this task we utilized RNA sequencing data from The Cancer  
144 Genome Atlas (TCGA) after stratifying patients by cancer type, *TP53* status  
145 and, where appropriate, cancer subtypes. The results indicate  
146 that *miR34a* asRNA and *miR34a* expression are strongly correlated in the  
147 vast majority of cancer types examined, both in the presence and absence of  
148 wild-type *TP53* (**Fig. 1c, Figure 1-Figure Supplement 1a**). The results also  
149 further confirm that the expression levels of both *miR34a* and its asRNA tend  
150 to be reduced in patients with nonsynonymous *TP53* mutations (**Figure 1-**  
151 **Figure Supplement 1b**).

152

153 Next, we aimed to gain a thorough understanding of *miR34a* asRNA's  
154 molecular characteristics and cellular localization. To experimentally  
155 determine the 3' termination site for the *miR34a* asRNA transcript we  
156 performed 3' rapid amplification of cDNA ends (RACE) using the U2OS  
157 osteosarcoma cell line that exhibited high endogenous levels  
158 of *miR34a* asRNA in the cell panel screening. By sequencing the cloned  
159 cDNA we determined that the transcripts 3' transcription termination site is  
160 525 base pairs upstream of the *LINC01759* transcript's annotated termination  
161 site (**Fig. 1d**). Next, we characterized the *miR34a* asRNA 5' transcription start  
162 site by carrying out a primer walk assay, i.e. a common reverse primer was  
163 placed in exon 2 and forward primers were gradually staggered upstream of  
164 the transcripts annotated start site (**Figure 1-Figure Supplement 2a**). Our  
165 results indicated that the 5' start site for *miR34a* asRNA is in fact

166 approximately 90bp (F11 primer) to 220bp (F12 primer) upstream of the  
167 annotated start site (**Fig. 1e**). Polyadenylation status was evaluated via cDNA  
168 synthesis with either random nanomers or oligoDT primers followed by semi-  
169 quantitative PCR with results indicating that the *miR34a* asRNA is  
170 polyadenylated although the unspliced form seems to only be in the polyA  
171 negative state (**Figure 1-Figure Supplement 2b**). We furthermore  
172 investigated the propensity of *miR34a* asRNA to be alternatively spliced,  
173 using PCR cloning and sequencing and found that the transcript is post-  
174 transcriptionally spliced to form multiple different isoforms (**Figure 1-Figure**  
175 **Supplement 2c**). \*\*\*make an additional supplementary figure showing spliced  
176 RNAseq reads\*\*\* Finally, to evaluate the cellular localization of *miR34a*  
177 asRNA we utilized RNA sequencing data from five cancer cell lines included  
178 in the ENCODE (Consortium 2012) project that had been fractionated into  
179 cytosolic and nuclear fractions. The analysis revealed that the *miR34a* asRNA  
180 transcript localizes to both the nucleus and cytoplasm but primarily resides in  
181 the nucleus (**Figure 1-Figure Supplement 2d**).

182

183 Finally, we utilized multiple approaches to evaluate the coding potential of  
184 the *miR34a* asRNA transcript. The Coding-Potential Assessment Tool is a  
185 bioinformatics-based tool that uses a logistic regression model to evaluate  
186 coding-potential by examining ORF length, ORF coverage, Fickett score and  
187 hexamer score (Wang et al. 2013). Results indicated that *miR34a* asRNA has  
188 a similar lack of coding capacity to the known non-coding  
189 transcripts *HOTAIR* and *XIST* and differs greatly when examining these  
190 parameters to the known coding transcripts  $\beta$ -actin, tubulin, and *MYC* (**Fig.**

191 **1F).** We further confirmed these results using the Coding-Potential Calculator  
192 that utilizes a support based machine-based classifier and accesses an  
193 alternate set of discriminatory features (**Figure 1-Figure Supplement 2e**)  
194 (Kong et al. 2007). \*\*\* We hope to be able to scan for peptides matching to  
195 miR34a asRNA in CPTAC and Geiger et al., 2012 before submission and will  
196 mention results here....\*\*\*

197

198 **TP53-mediated regulation of *miR34a* asRNA expression**

199 *miR34a* is a known downstream target of TP53 and has been previously  
200 shown to exhibit increased expression within multiple contexts of cellular  
201 stress. *miR34a* asRNA has also been shown to be induced upon TP53  
202 activation in several global analyses of p53-regulated lncRNAs (Rashi-Elkeles  
203 et al. 2014, Hunten et al. 2015, Leveille et al. 2015, Ashouri et al. 2016, Kim et  
204 al. 2017). To confirm these results in our biological system, we treated  
205 HEK293t, embryonic kidney cells, and HCT116, colorectal cancer cells, with  
206 the DNA damaging agent doxorubicin to activate TP53. QPCR-mediated  
207 measurement of both *miR34a* HG and asRNA indicated that their expression  
208 levels were increased in response to doxorubicin treatment in both cell lines  
209 (**Fig. 2a**). To assess if it is in fact *TP53* that is responsible for the increase  
210 in *miR34a* asRNA expression upon DNA damage, we  
211 treated *TP53*<sup>+/+</sup> and *TP53*<sup>-/-</sup> HCT116 cells with increasing concentrations of  
212 doxorubicin and monitored the expression of both *miR34a* HG and asRNA.  
213 We observed a dose-dependent increase in both *miR34a* HG and asRNA  
214 expression levels with increasing amounts of doxorubicin, indicating that  
215 these two transcripts are co-regulated, although, this effect was largely

216 abrogated in TP53<sup>-/-</sup> cells (**Fig. 2b**). These results indicate  
217 that *TP53* activation increases *miR34a* asRNA expression upon the induction  
218 of DNA damage. Nevertheless, *TP53*<sup>-/-</sup> cells also showed a dose dependent  
219 increase in both *miR34a* HG and asRNA, indicating that additional factors,  
220 other than *TP53*, are capable of initiating an increase in expression of both of  
221 these transcripts upon DNA damage.

222

223  
224  
225  
226  
227  
228  
229  
230  
231  
232  
233  
234  
235  
236

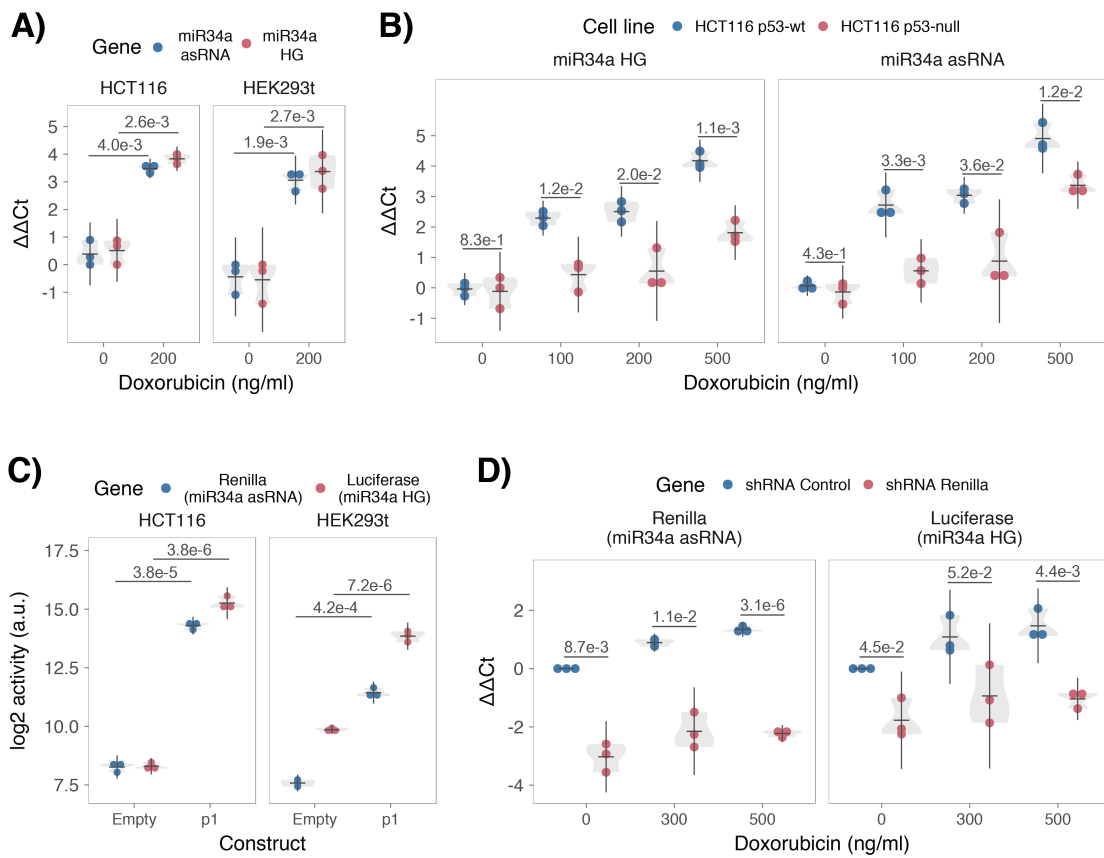


**Figure 2: TP53-mediated regulation of the *miR34a* locus.** **A)** Evaluating the effects of 24 hours of treatment with 200 ng/ml doxorubicin on *miR34a*asRNA and HG in HCT116 and HEK293t cells.\* **B)** Monitoring *miR34a* HG and asRNA expression levels during 24 hours doxorubicin treatment in *TP53*<sup>+/+</sup> and *TP53*<sup>-/-</sup> HCT116 cells.\* **C)** Quantification of luciferase and renilla levels after transfection of HCT116 and HEK293T cells with the p1 construct.\* **D)** HCT116 cells were co-transfected with the p1 construct and shRNA renilla or shRNA control and subsequently treated with increasing doses of doxorubicin. 24 hours post-treatment, cells were harvested and renilla and luciferase levels were measured using QPCR. Resulting p-values from statistical testing are shown above the shRenilla samples which were compared to the shRNA control using the respective treatment condition.\* Individual points represent results from independent experiments and the gray shadow indicates the density of those points. Error bars show the 95% CI, black horizontal lines represent the mean, and p-values are shown over long horizontal lines indicating the comparison tested.

237 The head-to head orientation of *miR34a* HG and asRNA, suggests that  
238 transcription is initiated from a single promoter in a bi-directional manner. To  
239 investigate whether *miR34a* HG and asRNA are transcribed from the same  
240 promoter as divergent transcripts, we cloned the *miR34a* HG promoter,  
241 including the *TP53* binding site, into a luciferase/renilla dual reporter vector  
242 which we hereafter refer to as p1 (**Figure 2-Figure Supplement 1a-b**). Upon  
243 transfection of p1 into HCT116 and HEK293t cell lines we observed increases  
244 in both luciferase and renilla indicating that *miR34a* HG and asRNA  
245 expression can be regulated by a single promoter contained within the p1  
246 construct (**Fig. 2c**).

247

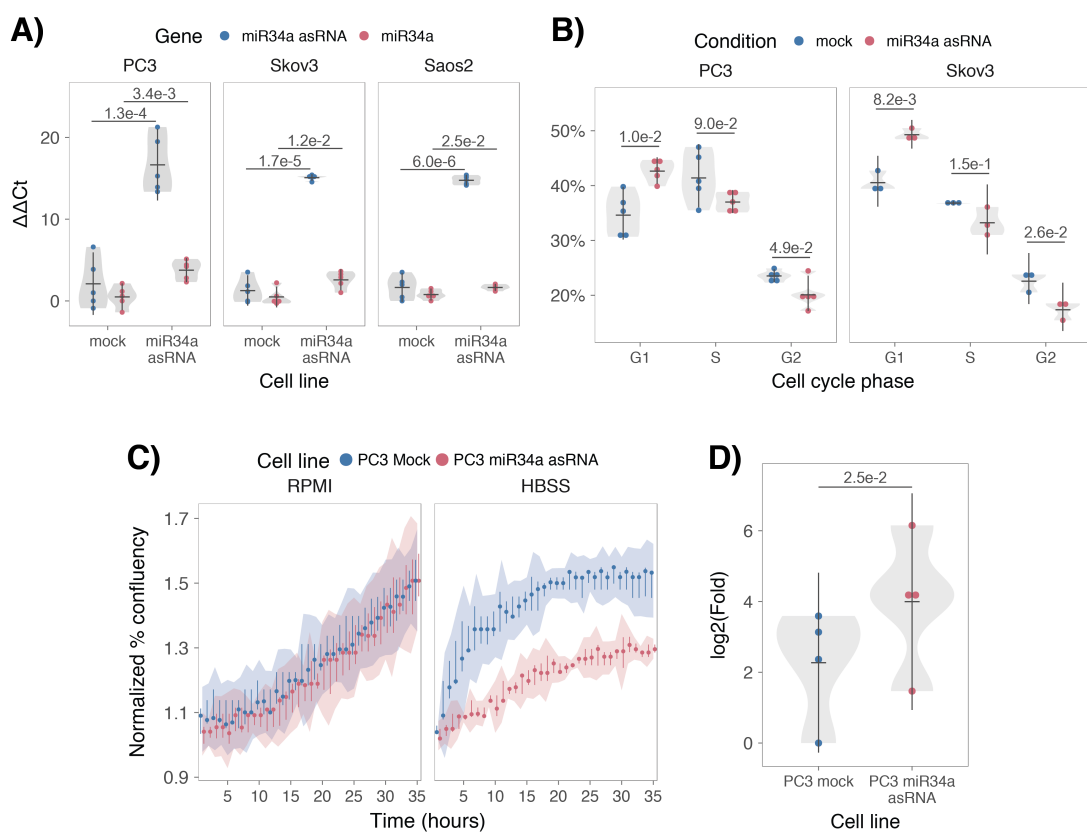
248 We hypothesized that *miR34a* asRNA may regulate *miR34a* HG levels and, in  
249 addition, that the overlapping regions of the sense and antisense transcripts  
250 may have a crucial role in mediating this regulation. Knock-down of  
251 endogenous *miR34a* asRNA is complicated by its various isoforms (**Figure 1-**  
252 **Figure Supplement 2c**). For this reason, we utilized the p1 construct to  
253 evaluate the regulatory role of the miR34a asRNA on miR34a HG.  
254 Accordingly, we first co-transfected the p1 construct, containing the  
255 overlapping region of the two transcripts, and a two different short hairpin (sh)  
256 RNAs targeting renilla into HEK293T cells and subsequently measured  
257 luciferase and renilla expression. The results indicated that shRNA-mediated  
258 knock down of the p1-renilla transcript (corresponding to *miR34a* asRNA)  
259 caused p1-luciferase (corresponding to *miR34a* HG) levels to concomitantly  
260 decrease (**Figure 2-Figure Supplement 2**). These results indicate  
261 that *miR34a* asRNA positively regulates levels of *miR34a* HG and that the

262 transcriptional product of the *miR34a* asRNA within in the p1 construct  
263 promotes a miR34a response. To further support these conclusions and  
264 better understand the role of miR34a asRNA during TP53 activation, *TP53<sup>+/+</sup>*  
265 HCT116 cells were co-transfected with p1 and shRNA renilla (2.1) and  
266 subsequently treated with increasing doses of doxorubicin. Again, the results  
267 showed a concomitant reduction in luciferase levels upon knock-down of p1-  
268 renilla i.e. the *miR34a* asRNA corresponding segment of the p1 transcript  
269 (**Fig. 2d**). Furthermore, the results showed that in the absence of p1-renilla,  
270 the expected induction of p1-luciferase in response to TP53 activation to DNA  
271 damage, is abrogated. Collectively these results indicate that *miR34a* asRNA  
272 positively regulates miR34a expression and is crucial for an appropriate  
273 TP53-mediated *miR34a* response to DNA damage.

274

275 ***miR34a* asRNA regulates its host gene independently of TP53**  
276 Despite the fact that TP53 regulates *miR34a* HG and asRNA expression, our  
277 results indicated that other factors are also able to regulate this locus (**Fig.**  
278 **2b**). Utilizing a lentiviral system, we stably over-expressed the *miR34a* asRNA  
279 transcript in three *TP53*-null cell lines, PC3 (prostate cancer), Saos2  
280 (osteogenic sarcoma), and Skov3 (adenocarcinoma). We first analyzed the  
281 levels of *miR34a* asRNA in these stable over-expression cell lines, compared  
282 to HEK293T cells, which have high endogenous levels of *miR34a* asRNA,  
283 finding that, on average, the over-expression was approximately 30-fold  
284 higher in the over-expression cell lines than in HEK293t cells. Due to the fact  
285 that *miR34a* asRNA can be up-regulated ~30-fold in response to DNA  
286 damage (**Fig. 2b**), we deemed this over-expression level to correspond to

287 physiologically relevant levels in cells encountering a stress stimulus, such as  
 288 DNA damage (**Figure 3-Figure Supplement 1**). Analysis of *miR34a* levels in  
 289 the *miR34a* asRNA over-expressing cell lines showed that *miR34a* asRNA  
 290 over-expression resulted in a concomitant increase in the expression  
 291 of *miR34a* in all three cell lines (**Fig. 3a**). These results indicate that, in the  
 292 absence of *TP53*, *miR34a* expression may be rescued by increasing the  
 293 levels of *miR34a* asRNA expression.



294

295 **Figure 3: miR34a asRNA positively regulates miR34a and its associated phenotypes.** **A)** QPCR-  
 296 mediated quantification of *miR34a* expression in cell lines stably over-  
 297 expressing *miR34a* asRNA.\* **B)** Cell cycle analysis comparing stably over-expressing *miR34a* asRNA  
 298 cells to the respective mock expressing cells.\* **C)** Analysis of cellular growth over time in *miR34a*  
 299 asRNA over-expressing PC3 cells. Points represent the median from 3 independent experiments, the  
 300 colored shadows indicate the 95% confidence interval, and vertical lines show the minimum and  
 301 maximum values obtained from the three biological replicates. **D)** Differential phosphorylated  
 302 polymerase II binding in *miR34a* asRNA over-expressing PC3 cells.\* Individual points represent  
 303 results from independent experiments and the gray shadow indicates the density of those points. Error  
 304 bars show the 95% CI, black horizontal lines represent the mean, and p-values are shown over long  
 305 horizontal lines indicating the comparison tested.  
 306

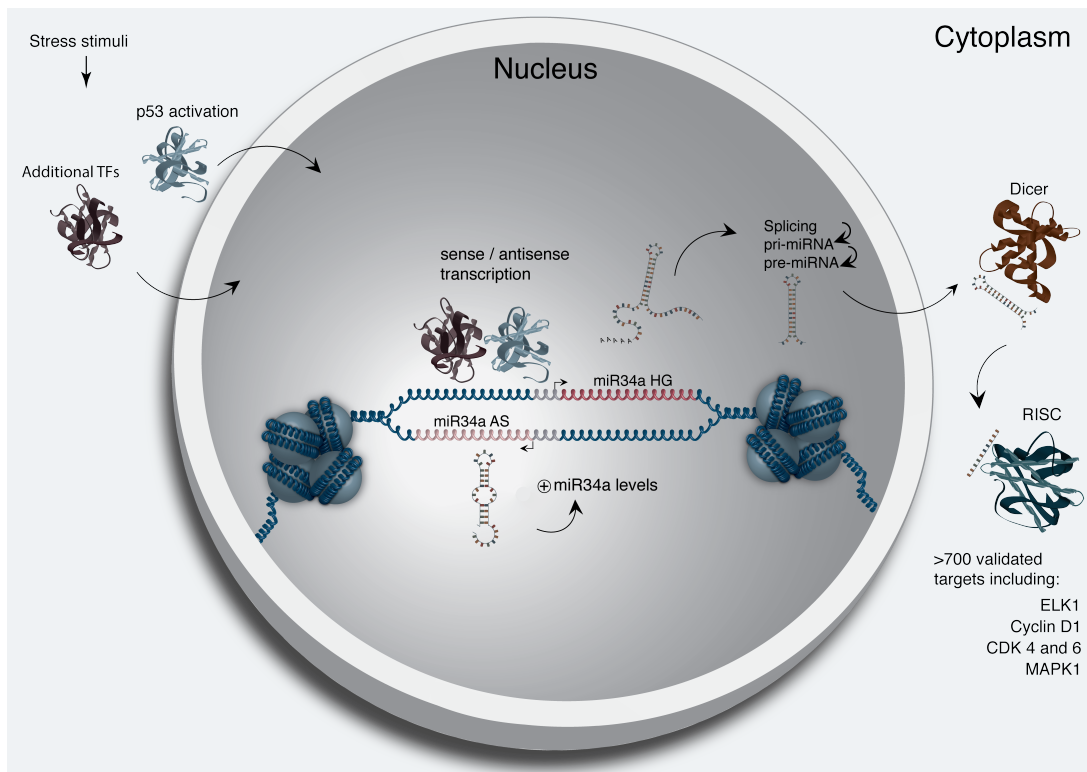
307 *miR34a* has been previously shown to regulate cell cycle progression, with  
308 *miR34a* induction causing G1 arrest. Cell cycle analysis via determination of  
309 DNA content showed a significant increase in G1 phase cells in the PC3 and  
310 Skov3 *miR34a* asRNA over-expressing cell lines, indicative of G1 arrest, as  
311 well as, a significant decrease of cells in G2 phase (**Fig. 3b**). *miR34a*'s effects  
312 on the cell cycle are mediated by its ability to target cell cycle regulators such  
313 as cyclin D1 (*CCND1*) (Sun et al. 2008). We therefore sought to determine if  
314 the *miR34a* asRNA over-expressing cell lines exhibited effects on this  
315 known *miR34a* target. Quantification of both *CCND1* RNA expression (**Figure**  
316 **3-Figure Supplement 2a**) and protein levels (**Figure 3-Figure Supplement**  
317 **2b**) in the PC3 *miR34a* asRNA over-expressing cell line showed a significant  
318 decrease of *CCND1* levels compared to the mock control.

319  
320 *miR34a* is also a well known inhibitor of cellular growth via its ability to  
321 regulate growth factor signaling. Furthermore, starvation has been shown to  
322 induce *miR34a* expression that down-regulates multiple targets that aid in the  
323 phosphorylation of multiple pro-survival growth factors (Lal et al. 2011). We  
324 further interrogated the effects of *miR34a* asRNA over-expression by  
325 investigating the growth of the cells in both normal and starvation conditions  
326 by measuring confluency over a 35-hour period. Under normal growth  
327 conditions there is a small but significant reduction ( $p = 3.0\text{e-}8$ ) in confluency  
328 in the *miR34a* asRNA over-expressing cell lines, these effects on cell growth  
329 are drastically increased in starvation conditions ( $p = 9.5\text{e-}67$ ). This is in  
330 accordance with our previous results, and suggests that *miR34a* asRNA-  
331 mediated increases in *miR34a* expression are crucial under conditions of

332 stress and necessary for the initiation of an appropriate cellular response. In  
333 summary, we find that over-expression of *miR34a* asRNA is sufficient to  
334 increase *miR34a* expression and gives rise to known phenotypes observed  
335 with increased *miR34a* expression.

336

337 Antisense RNAs have been reported to mediate their effects both via  
338 transcriptional and post-transcriptional mechanisms. Due to the fact that  
339 *miR34a* expression is undetected in wild type PC3 cells but, upon over-  
340 expression of *miR34a* asRNA, increases to detectable levels, we  
341 hypothesized that *miR34a* asRNA is capable of regulating *miR34a* expression  
342 levels via a transcriptional mechanism. To ascertain if this is actually the case,  
343 we performed chromatin immunoprecipitation (ChIP) for phosphorylated  
344 polymerase II (polII) at the *miR34a* HG promoter in both *miR34a* asRNA over-  
345 expressing and mock control cell lines. Our results indicated a clear increase  
346 in phosphorylated polII binding at the *miR34a* promoter upon *miR34a* asRNA  
347 over-expression indicating *miR34a* asRNA's ability to regulate *miR34a* levels  
348 on a transcriptional level (**Fig. 3d**).



349

350 **Figure 4: A graphical summary of the proposed *miR34a* asRNA function.** Stress stimuli,  
 351 originating in the cytoplasm or nucleus, activates *TP53* as well as additional factors. These factors then  
 352 bind to the *miR34a* promoter and drive transcription of the sense and antisense strands. *miR34a* asRNA  
 353 serves to increase the levels of *miR34a* HG transcription via an unknown mechanism. *miR34a* HG  
 354 then, in turn, is then spliced, processed by the RNase III enzyme Drosha, and exported to the  
 355 cytoplasm. The *miR34a* pre-miRNA then binds to Dicer where the hair-pin loop is cleaved and  
 356 mature *miR34a* is formed. Binding of the mature *miR34a* miRNA to the RISC complex then allows it  
 357 to bind and repress its targets.  
 358

359 \*\*\*You can add polII in this figure\*\*\*

360 **Discussion**

361  
362 Multiple studies have previously shown asRNAs to be crucial for the  
363 appropriate regulation of cancer-associated protein-coding genes and that  
364 their dys-regulation can lead to perturbation of tumor suppressive and  
365 oncogenic pathways, as well as, cancer-related phenotypes (Yu et al. 2008,  
366 Yap et al. 2010, Serviss et al. 2014, Balbin et al. 2015). Here we show that  
367 asRNAs are also capable of regulating cancer-associated miRNAs resulting in  
368 similar consequences as protein-coding gene dys-regulation (**Fig. 4**).  
369 Interestingly, we show that, both in the presence and absence of  
370 *TP53*, *miR34a* asRNA provides an additional regulatory level and functions by  
371 mediating the increase of *miR34a* expression in both homeostasis and upon  
372 encountering multiple forms of cellular stress. Furthermore, we find that  
373 *miR34a* asRNA-mediated increases in *miR34a* expression levels are sufficient  
374 to drive the appropriate cellular responses to multiple forms of stress stimuli  
375 that are encountered (**Fig. 2d and Fig. 3c**). Previous studies have utilized  
376 various molecular biology methods to up regulate *miR34a* expression in a p53  
377 deficient background showing similar phenotypic outcomes but, to our  
378 knowledge, this is the first example of an endogenous mechanism by which  
379 this can be achieved (Liu et al. 2011, Ahn et al. 2012, Yang et al. 2012,  
380 Stahlhut et al. 2015, Wang et al. 2015).

381

382 In agreement with previous studies, we demonstrate that upon encountering  
383 various types of cellular stress, TP53 in concert with additional factors bind  
384 and initiate transcription at the *miR34a* locus, thus increasing the levels of  
385 *miR34a* and, in addition, *miR34a* asRNA. We hypothesize that *miR34a*

386 asRNA may form a positive feedback for *miR34a* expression whereby *miR34a*  
387 asRNA serves as a scaffold for the recruitment of additional factors that  
388 facilitate polIII-mediated transcription, thus, increasing the expression of  
389 *miR34a* and driving the cell towards a reduction in growth factor signaling,  
390 senescence, and eventually apoptosis. On the other hand, in cells without a  
391 functional *TP53*, other factors, which typically act independently or in concert  
392 with *TP53*, may initiate transcription of the *miR34a* locus. We believe that  
393 *miR34a* asRNA could potentially be interacting directly with one of these  
394 additional factors and recruiting it to the *miR34a* locus in order to drive  
395 *miR34a* transcription. This is especially plausible due to head-to-head  
396 orientation of the *miR34a* HG and asRNA, causing sequence complementarity  
397 between the RNA and the promoter DNA. Previous reports have illustrated  
398 also illustrated the ability of asRNAs to form hybrid DNA:RNA R-loops and,  
399 thus, facilitate an open chromatin structure and the transcription of the sense  
400 gene (Boque-Sastre et al. 2015). The fact that the p1 construct only contains  
401 a small portion of the *miR34a* asRNA transcript indicates that this portion is  
402 sufficient to give rise to at least a partial *miR34a* inducing response may  
403 indicate that *miR34a* asRNA may be able to facilitate *miR34a* expression  
404 independent of additional factors. Nevertheless, further work will need to be  
405 performed to ascertain the mechanism that is utilized in the case of *miR34a*  
406 asRNA.

407  
408 An unannotated transcript, *Lnc34a*, arising from the antisense orientation of  
409 the *miR34a* locus and with a transcription start site >250 bp upstream of the  
410 annotated *miR34a* asRNAs start site, has been previously reported in a study

411 examining colorectal cancer (Wang et al. 2016). Among the findings in Wang  
412 et al. the authors discover that *Lnc34a* negatively regulates miR34a  
413 expression via recruitment of *DNMT3a*, *PHB2*, and *HDAC1* to the *miR34a*  
414 promoter. Although the *Lnc34a* and *miR34a* asRNA transcripts share some  
415 sequence similarity, we believe them to be separate RNAs that are,  
416 potentially, different isoforms of the same gene. Furthermore, *Lnc34a* may be  
417 highly context dependent and potentially only expressed at biologically  
418 significant levels in colon cancer stem cells, or other stem-like cells, in  
419 agreement with the conclusions drawn in the paper. We thoroughly address  
420 our reasons for these beliefs and give appropriate supporting evidence in  
421 (**Supplementary Results 4**). The fact that *Lnc34a* and *miR34a* asRNA would  
422 appear to have opposing roles in their regulation of *miR34a* further underlines  
423 the complexity of the regulation at this locus.

424

425 The fact that the p1 construct only contains a small portion of the *miR34a*  
426 asRNA transcript indicates that this portion is sufficient to give rise to at least  
427 a partial *miR34a* inducing response thus providing a potential pathway  
428 towards oligonucleotide-mediated therapies (**Fig 2d, Figure 2-Figure**  
429 **Supplement 2a**). In fact, clinical trials utilizing miR34a replacement therapy  
430 have previously been conducted but, disappointingly, were terminated after  
431 adverse side effects of an immunological nature were observed in several of  
432 the patients (Slabakova et al. 2017). Although it is not presently clear if these  
433 side effects were caused by *miR34a* or the liposomal carrier used to deliver  
434 the miRNA, the multitude of evidence indicating *miR34a*'s crucial role in  
435 oncogenesis still makes its therapeutic induction an interesting strategy for

436 therapy and needs further investigation.

437

438 In summary, our results indicate that *miR34a* asRNA is a vital player in the  
439 regulation of *miR34a* and is especially important in contexts where cellular  
440 stresses are encountered. Due to the fact that many of these stress stimuli  
441 are strongly associated with cancer, we believe *miR34a* asRNA's ability to  
442 fine-tune *miR34a* expression levels to be especially crucial in tumorigenesis.

443

#### 444 **Materials and Methods**

##### 445 **Cell Culture**

446 All cell lines were cultured at 5% CO<sub>2</sub> and 37° C with HEK293T, Saos2, and  
447 Skov3 cells cultured in DMEM high glucose (GE Healthcare Life Sciences,  
448 Hyclone, UT, USA, Cat# SH30081), HCT116 and U2OS cells in McCoy's 5a  
449 (ThermoFisher Scientific, MA, USA, Cat# SH30200), and PC3 cells in RPMI  
450 (GE Healthcare Life Sciences, Hyclone, Cat# SH3009602) and 2 mM L-  
451 glutamine (GE Healthcare Life Sciences, Hyclone, Cat# SH3003402). All  
452 growth mediums were supplemented with 10% heat-inactivated FBS  
453 (ThermoFisher Scientific, Gibco, Cat# 12657029) and 50 µg/ml of  
454 streptomycin (ThermoFisher Scientific, Gibco, Cat# 15140122) and 50 µg/ml  
455 of penicillin (ThermoFisher Scientific, Gibco, Cat# 15140122).

##### 456 457 **Bioinformatics and Data Availability**

458 The USCS genome browser (Kent et al. 2002) was utilized for the  
459 bioinformatic evaluation of antisense transcription utilizing the RefSeq  
460 (O'Leary et al. 2016) gene annotation track.

461

462 All raw experimental data, code used for analysis, and supplementary  
463 methods are available for review at ([Serviss 2017](#)) and are provided as an R  
464 package. All analysis took place using the R statistical programming language  
465 (Team 2017) using multiple external packages that are all documented in the  
466 package associated with the article (Wilkins , Chang 2014, Wickham 2014,  
467 Wickham 2016, Allaire et al. 2017, Arnold 2017, Wickham 2017, Wickham  
468 2017, Wickham 2017, Xiao 2017, Xie 2017). The package facilitates  
469 replication of the operating system and package versions used for the original  
470 analysis, reproduction of each individual figure included in the article, and  
471 easy review of the code used for all steps of the analysis, from raw-data to  
472 figure.

473

#### 474 **Coding Potential**

475 Protein-coding capacity was evaluated using the Coding-potential  
476 Assessment Tool (Wang et al. 2013) and Coding-potential Calculator (Kong et  
477 al. 2007) with default settings. Transcript sequences for use with Coding-  
478 potential Assessment Tool were downloaded from the UCSC genome  
479 browser using the Ensembl  
480 accessions: *HOTAIR* (ENST00000455246), *XIST* (ENST00000429829), β-  
481 actin (ENST00000331789), Tubulin (ENST00000427480),  
482 and *MYC* (ENST00000377970). Transcript sequences for use with Coding-  
483 potential Calculator were downloaded from the UCSC genome browser using  
484 the following IDs: *HOTAIR* (uc031qho.1), β-actin (uc003soq.4).

485

#### 486 **shRNAs**

487 shRNA-expressing constructs were cloned into the U6M2 construct using the  
488 BgIII and KpnI restriction sites as previously described (Amarzguioui et al.  
489 2005). shRNA constructs were transfected using Lipofectamine 2000 or 3000  
490 (ThermoFisher Scientific, Cat# 12566014 and L3000015). The sequence  
491 targeting renilla is as follows: AAT ACA CCG CGC TAC TGG C.

492

#### 493 **Lentiviral Particle production, infection, and selection**

494 Lentivirus production was performed as previously described in (Turner et al.  
495 2012). Briefly, HEK293T cells were transfected with viral and expression  
496 constructs using Lipofectamine 2000 (ThermoFisher Scientific, Cat#  
497 12566014), after which viral supernatants were harvested 48 and 72 hours  
498 post-transfection. Viral particles were concentrated using PEG-IT solution  
499 (Systems Biosciences, CA, USA, Cat# LV825A-1) according to the  
500 manufacturer's recommendations. HEK293T cells were used for virus titration  
501 and GFP expression was evaluated 72hrs post-infection via flow cytometry  
502 (LSRII, BD Biosciences, CA, USA) after which TU/ml was calculated.

503

504 Stable lines were generated by infecting cells with a multiplicity of infection of  
505 1 after which 1-2 µM mycophenolic acid (Merck, NJ, USA, Cat# M5255)  
506 selection was initiated 48 hours post-infection. Cells were expanded as the  
507 selection process was monitored via flow cytometry analysis (LSRII, BD  
508 Biosciences) of GFP and selection was terminated once > 90% of the cells  
509 were GFP positive.

510

#### 511 **Western Blotting**

512 Samples were lysed in 50 mM Tris-HCl (Sigma Aldrich, MO, USA, Cat#  
513 T2663), pH 7.4, 1% NP-40 (Sigma Aldrich, Cat# I8896), 150 mM NaCl (Sigma  
514 Aldrich, Cat# S5886), 1 mM EDTA (Promega, WI, USA, Cat# V4231), 1%  
515 glycerol (Sigma Aldrich, Cat# G5516), 100 µM vanadate (), protease inhibitor  
516 cocktail (Roche Diagnostics, Basel, Switzerland, Cat# 004693159001) and  
517 PhosSTOP (Roche Diagnostics, Cat# 04906837001). Lysates were subjected  
518 to SDS-PAGE and transferred to PVDF membranes. The proteins were  
519 detected by western blot analysis by using an enhanced chemiluminescence  
520 system (Western Lightning–ECL, PerkinElmer, Cat# NEL103001EA).  
521 Antibodies used were specific for CCND1 1:1000 (Cell Signaling, Cat# 2926),  
522 and β-actin 1:5000 (Sigma-Aldrich, Cat# A5441). All western blot  
523 quantifications were performed using ImageJ (Schneider et al. 2012).

524

525 **Generation of U6-expressed miR34a AS Lentiviral Constructs**

526 The U6 promoter was amplified from the U6M2 cloning plasmid (Amarzguioui  
527 et al. 2005) and ligated into the Not1 restriction site of the pHIV7-IMPDH2  
528 vector (Turner et al. 2012). miR43a asRNA was PCR amplified and  
529 subsequently cloned into the Nhe1 and Pac1 restriction sites in the pHIV7-  
530 IMPDH2-U6 plasmid.

531

532 **Promoter Activity**

533 Cells were co-transfected with the renilla/firefly bidirectional promoter  
534 construct (Polson et al. 2011) and GFP by using Lipofectamine 2000 (Life  
535 Technologies, Cat# 12566014). The expression of GFP and luminescence  
536 was measured 24 h post transfection by using the Dual-Glo Luciferase Assay

537 System (Promega, Cat# E2920) and detected by the GloMax-Multi+ Detection  
538 System (Promega, Cat# SA3030). The expression of luminescence was  
539 normalized to GFP.

540

541 **RNA Extraction and cDNA Synthesis**

542 For downstream SYBR green applications, RNA was extracted using the  
543 RNeasy mini kit (Qiagen, Venlo, Netherlands, Cat# 74106) and subsequently  
544 treated with DNase (Ambion Turbo DNA-free, ThermoFisher Scientific, Cat#  
545 AM1907). 500ng RNA was used for cDNA synthesis using MuMLV  
546 (ThermoFisher Scientific, Cat# 28025013) and a 1:1 mix of oligo(dT) and  
547 random nanomers.

548

549 For analysis of miRNA expression with Taqman, samples were isolated with  
550 TRIzol reagent (ThermoFisher Scientific, Cat# 15596018) and further  
551 processed with the miRNeasy kit (Qiagen, Cat# 74106). cDNA synthesis was  
552 performed using the TaqMan MicroRNA Reverse Transcription Kit  
553 (ThermoFisher Scientific, Cat# 4366597) using the corresponding oligos  
554 according to the manufacturer's recommendations.

555

556 **QPCR and PCR**

557 PCR was performed using the KAPA2G Fast HotStart ReadyMix PCR Kit  
558 (Kapa Biosystems, MA, USA, Cat# KK5601) with corresponding primers.  
559 QPCR was carried out using KAPA 2G SYBRGreen (Kapa Biosystems, Cat#  
560 KK4602) using the Applied Biosystems 7900HT machine with the cycling  
561 conditions: 95 °C for 3 min, 95 °C for 3 s, 60 °C for 30 s.

562  
563 QPCR for miRNA expression analysis was performed according to the primer  
564 probe set manufacturers recommendations (ThermoFisher Scientific) and  
565 using the TaqMan Universal PCR Master Mix (ThermoFisher Scientific, Cat#  
566 4304437) with the same cycling scheme as above. Primer and probe sets for  
567 TaqMan were also purchased from ThermoFisher Scientific (Life  
568 Technologies at time of purchase, TaqMan® MicroRNA Assay, hsa-miR-34a,  
569 human, Cat# 4440887, Assay ID: 000426 and Control miRNA Assay, RNU48,  
570 human, Cat# 4440887, Assay ID: 001006).

571  
572 Primers for all PCR-based experiments are listed in **Supplementary**  
573 **Document 2** and arranged by figure.

574  
575 **Bi-directional Promoter Cloning**  
576 The overlapping region (p1) corresponds with the sequence previously  
577 published as the TP53 binding site in (Raver-Shapira et al. 2007) which we  
578 synthesized and cloned into the pLucRluc construct (Polson et al. 2011).

579  
580 **Cell Cycle Distribution**  
581 Cells were washed in PBS and fixed in 4% paraformaldehyde at room  
582 temperature overnight. Paraformaldehyde was removed, and cells were re-  
583 suspended in 95% EtOH. The samples were then rehydrated in distilled  
584 water, stained with DAPI and analyzed by flow cytometry on a LSRII (BD  
585 Biosciences) machine. Resulting cell cycle phases were quantified using the  
586 ModFit software (Verity Software House, ME, USA).

587

588 **3' Rapid Amplification of cDNA Ends**

589 3'-RACE was performed as described as previously in (Johnsson et al. 2013).  
590 Briefly, U2OS cell RNA was polyA-tailed using yeast polyA polymerase  
591 (ThermoFisher Scientific, Cat# 74225Z25KU) after which cDNA was  
592 synthesized using oligo(dT) primers. Nested-PCR was performed first using a  
593 forward primer in miR34a asRNA exon 1 and a tailed oligo(dT) primer  
594 followed by a second PCR using an alternate miR34a asRNA exon 1 primer  
595 and a reverse primer binding to the tail of the previously used oligo(dT)  
596 primer. PCR products were gel purified and cloned the Strata Clone Kit  
597 (Agilent Technologies, CA, USA, Cat# 240205), and sequenced.

598

599 **Chromatin Immunoprecipitation**

600 The ChIP was performed as previously described in (Johnsson et al. 2013)  
601 with the following modifications. Cells were crosslinked in 1% formaldehyde  
602 (Merck, Cat# 1040039025), quenched with 0.125M glycine (Sigma Aldrich,  
603 Cat# G7126), and lysed in cell lysis buffer comprised of: 5mM PIPES (Sigma  
604 Aldrich, Cat# 80635), 85mM KCL (Merck, Cat# 4936), 0.5% NP40 (Sigma  
605 Aldrich, Cat# I8896), protease inhibitor (Roche Diagnostics, Cat#  
606 004693159001). Samples were then sonicated in 50mM TRIS-HCL pH 8.0  
607 (Sigma Aldrich, MO, USA, Cat# T2663) 10mM EDTA (Promega, WI, USA,  
608 Cat# V4231), 1% SDS (ThermoFisher Scientific, Cat# AM9822), and protease  
609 inhibitor (Roche Diagnostics, Cat# 004693159001) using a Bioruptor  
610 Sonicator (Diagenode, NJ, USA). Samples were incubated over night at 4°C  
611 with the *polII* antibody (Abcam, Cambridge, UK, Cat# ab5095) and

612 subsequently pulled down with Salmon Sperm DNA/Protein A Agarose  
613 (Millipore, Cat# 16-157) beads. DNA was eluted in an elution buffer of 1%  
614 SDS (ThermoFisher Scientific, Cat# AM9822) 100mM NaHCO3 (Sigma  
615 Aldrich, Cat# 71631), followed by reverse crosslinking, RNaseA  
616 (ThermoFisher Scientific, Cat# 1692412) and protease K (New England  
617 Biolabs, MA, USA, Cat# P8107S) treatment. The DNA was eluted using  
618 Qiagen PCR purification kit (Cat# 28106).

619

## 620 **Confluency Analysis**

621 Cells were incubated in the Spark Multimode Microplate (Tecan) reader for 48  
622 hours at 37°C with 5% CO<sub>2</sub> in a humidity chamber. Confluency was  
623 measured every hour using bright-field microscopy and the percentage of  
624 confluency was reported via the plate reader's inbuilt algorithm. Percentage of  
625 confluency was normalized to the control sample in each condition (shown in  
626 figure) and then ranked. The rank was then used to construct a linear model of  
627 the dependency of the rank on the time and cell lines variables for each  
628 growth condition. Reported p-values are derived from the t-test, testing the  
629 null hypothesis that the coefficient estimate of the cell line variable is equal to  
630 0.

631

## 632 **Pharmacological Compounds**

633 Doxorubicin was purchased from Teva (cat. nr. 021361).

634

## 635 **Cellular Localization Analysis**

636 Quantified RNAseq data from 11 cell lines from the GRCh38 assembly was

637 downloaded from the ENCODE project database and quantifications for  
638 miR34a asRNA (ENSG00000234546), GAPDH (ENSG00000111640), and  
639 MALAT1 (ENSG00000251562) were extracted. Cell lines for which data was  
640 downloaded include: A549, GM12878, HeLa-S3, HepG2, HT1080, K562  
641 MCF-7, NCI-H460, SK-MEL-5, SK-N-DZ, SK-N-SH. Initial exploratory analysis  
642 revealed that several cell lines should be removed from the analysis due to a)  
643 a larger proportion of GAPDH in the nucleus than cytoplasm or b) variation of  
644 miR34a asRNA expression is too large to draw conclusions, or c) they have  
645 no or low (<6 TPM) miR34a asRNA expression. Furthermore, only  
646 polyadenylated libraries were used in the final analysis, due to the fact that  
647 the cellular compartment enrichment was improved in these samples. All  
648 analyzed genes are reported to be polyadenylated. In addition, only samples  
649 with 2 biological replicates were retained. For each cell type, gene, and  
650 biological replicate the fraction of transcripts per million (TPM) in each cellular  
651 compartment was calculated as the fraction of TPM in the specific  
652 compartment by the total TPM. The mean and standard deviation for the  
653 fraction was subsequently calculated for each cell type and cellular  
654 compartment and this information was represented in the final figure.

655

## 656 **CAGE Analysis**

657 All available CAGE data from the ENCODE project (Consortium 2012) for 36  
658 cell lines was downloaded from the UCSC genome browser (Kent et al. 2002)  
659 for genome version hg19. Of these, 28 cell lines had CAGE transcription start  
660 sites (TSS) mapping to the plus strand of chromosome 1 and in regions  
661 corresponding to 200 base pairs upstream of the *lnc34a* start site (9241796 -

662 200) and 200 base pairs upstream of the GENCODE  
663 annotated *miR34a* asRNA start site (9242263 + 200). These cell lines  
664 included: HFDPC, H1-hESC, HMEpC, HAoEC, HPIEpC, HSaVEC, GM12878,  
665 hMSC-BM, HUVEC, AG04450, hMSC-UC, IMR90, NHDF, SK-N-SH\_RA, BJ,  
666 HOB, HPC-PL, HAoAF, NHEK, HVMF, HWP, MCF-7, HepG2, hMSC-AT,  
667 NHEM.f\_M2, SkMC, NHEM\_M2, and HCH. In total 74 samples were included.  
668 17 samples were polyA-, 47 samples were polyA+, and 10 samples were total  
669 RNA. In addition, 34 samples were whole cell, 15 enriched for the cytosolic  
670 fraction, 15 enriched for the nucleolus, and 15 enriched for the nucleus. All  
671 CAGE transcription start sites were plotted and the RPKM of the individual  
672 reads was used to color each read to indicate their relative abundance. In  
673 cases where CAGE TSS spanned identical regions, the RPMKs of the regions  
674 were summed and represented as one CAGE TSS in the figure. In addition, a  
675 density plot shows the distribution of the CAGE reads in the specified  
676 interval.

677

### 678 **Splice Junction Analysis**

679 All available whole cell (i.e. non-fractionated) spliced read data originating  
680 from the Cold Spring Harbor Lab in the ENCODE project (Consortium 2012)  
681 for 38 cell lines was downloaded from the UCSC genome browser (Kent et al.  
682 2002). Of these cell lines, 36 had spliced reads mapping to the plus strand of  
683 chromosome 1 and in the region between the *lnc34a* start (9241796) and  
684 transcription termination (9257102) site (note that *miR34a* asRNA resides  
685 totally within this region). Splice junctions from the following cell lines were  
686 included in the final figure: A549, Ag04450, Bj, CD20, CD34 mobilized,

687 Gm12878, H1hesc, Haoaf, Haoec, Hch, Helas3, Hepg2, Hfdpc, Hmec,  
688 Hmepc, Hmscat, Hmscbm, Hmscuc, Hob, Hpcpl, Hpiepc, Hsavec, Hsmm,  
689 Huvec, Hvmf, Hwp, Imr90, Mcf7, Monocd14, Nhdf, Nhek, Nhjemfm2,  
690 Nhemm2, Nhlf, Skmc, and Sknsh. All splice junctions were included in the  
691 figure and colored according to the number of reads corresponding to each. In  
692 cases where identical reads were detected multiple times, the read count was  
693 summed and represented as one read in the figure.

694

695 **Correlation analysis**

696 Erik/Jimmy should probably take this.

697  
698 **Acknowledgments**  
699

700 **Competing Interests**

701  
702 The authors declare no competing interests.  
703

704 **Figure Supplements**

705  
706 List figure supplements here!

707

708 **Supplementary Figures**

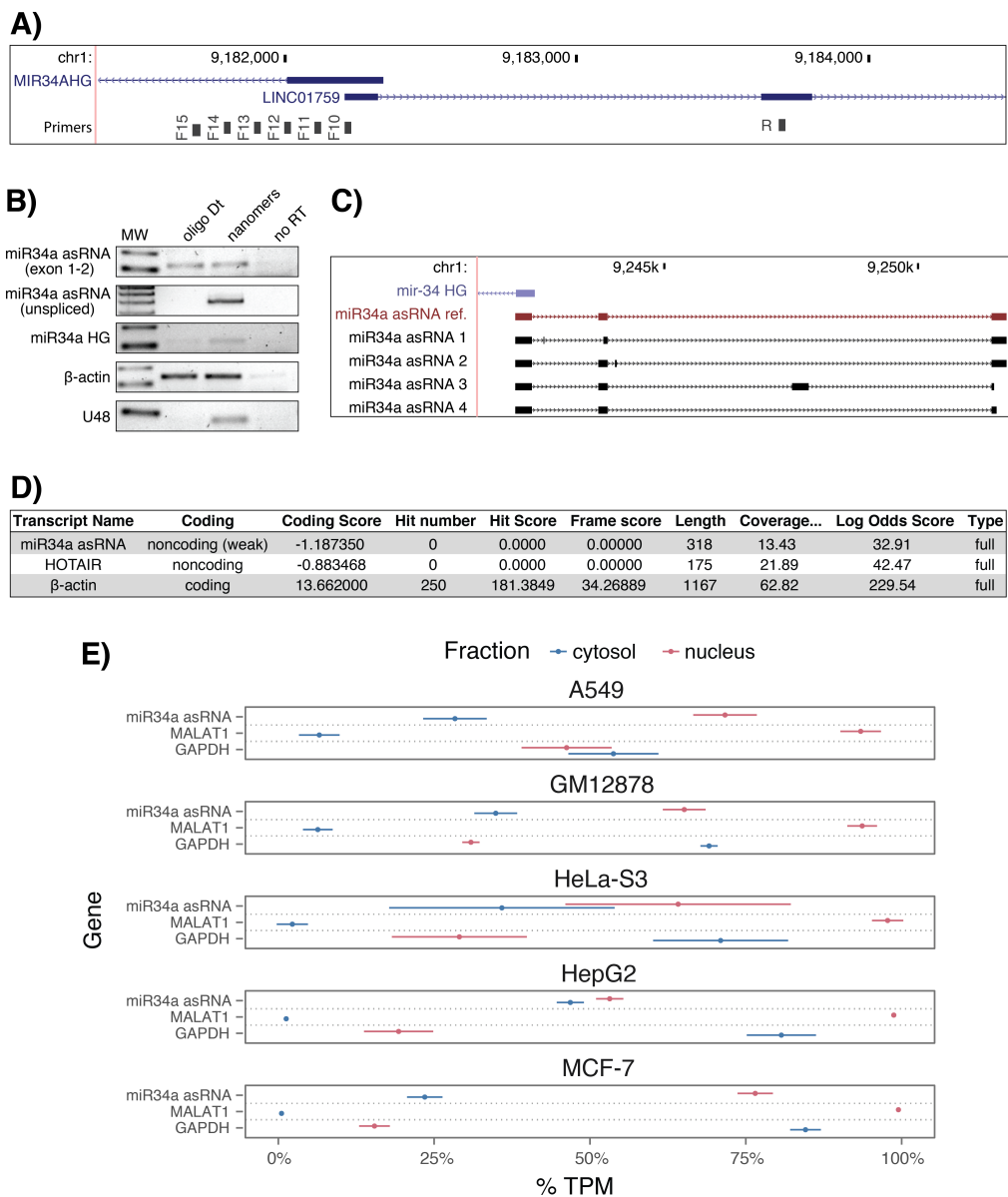
709  
710

A)

| cancer     | all n | all rho  | all p    | TP53wt n | TP53wt rho | TP53wt p | TP53mut n | TP53mut rho | TP53mut p |
|------------|-------|----------|----------|----------|------------|----------|-----------|-------------|-----------|
| ACC        | 10    | 5.52e-01 | 1.04e-01 | 10       | 5.52e-01   | 1.04e-01 | NA        | NA          | NA        |
| BLCA       | 228   | 5.15e-01 | 7.89e-17 | 134      | 4.53e-01   | 3.86e-08 | 94        | 4.27e-01    | 1.73e-05  |
| BRCA Basal | 42    | 5.74e-01 | 9.54e-05 | 10       | 6.24e-01   | 6.02e-02 | 32        | 5.74e-01    | 7.41e-04  |
| BRCA Her2  | 44    | 1.47e-01 | 3.39e-01 | 12       | 2.24e-01   | 4.85e-01 | 32        | 6.82e-02    | 7.10e-01  |
| BRCA LumA  | 199   | 3.41e-01 | 8.22e-07 | 177      | 3.43e-01   | 2.96e-06 | 22        | 4.86e-01    | 2.31e-02  |
| BRCA LumB  | 70    | 1.71e-01 | 1.57e-01 | 61       | 1.48e-01   | 2.53e-01 | 9         | 1.67e-01    | 6.78e-01  |
| CESC       | 156   | 1.39e-01 | 8.37e-02 | 145      | 1.60e-01   | 5.45e-02 | 11        | -4.55e-02   | 9.03e-01  |
| HNSC       | 313   | 5.37e-01 | 8.38e-25 | 123      | 6.08e-01   | 0.00e+00 | 190       | 4.47e-01    | 9.68e-11  |
| KICH       | 5     | 6.00e-01 | 3.50e-01 | 5        | 6.00e-01   | 3.50e-01 | NA        | NA          | NA        |
| KIRC       | 142   | 3.49e-01 | 2.06e-05 | 141      | 3.37e-01   | 4.41e-05 | NA        | NA          | NA        |
| KIRP       | 167   | 4.51e-01 | 9.16e-10 | 163      | 4.48e-01   | 2.04e-09 | 4         | 8.00e-01    | 3.33e-01  |
| LGG        | 271   | 6.33e-01 | 9.92e-32 | 76       | 7.28e-01   | 0.00e+00 | 195       | 3.87e-01    | 2.26e-08  |
| LIHC       | 153   | 5.63e-01 | 3.64e-14 | 114      | 5.16e-01   | 4.18e-09 | 39        | 4.55e-01    | 3.95e-03  |
| LUAD       | 234   | 2.82e-01 | 1.15e-05 | 128      | 3.61e-01   | 2.87e-05 | 106       | 2.27e-01    | 1.91e-02  |
| LUSC       | 139   | 2.29e-01 | 6.74e-03 | 42       | 4.17e-02   | 7.93e-01 | 97        | 3.29e-01    | 9.91e-04  |
| OV         | 56    | 2.33e-01 | 8.37e-02 | 10       | 8.42e-01   | 4.46e-03 | 46        | 1.46e-01    | 3.31e-01  |
| PRAD       | 413   | 4.66e-01 | 1.33e-23 | 375      | 4.59e-01   | 6.13e-21 | 38        | 4.50e-01    | 4.58e-03  |
| SKCM       | 165   | 6.48e-01 | 5.43e-21 | 152      | 6.10e-01   | 7.85e-17 | 13        | 4.34e-01    | 1.40e-01  |
| STAD       | 225   | 3.72e-01 | 8.23e-09 | 145      | 3.67e-01   | 5.71e-06 | 80        | 4.20e-01    | 1.03e-04  |
| THCA       | 469   | 4.58e-01 | 1.07e-25 | 467      | 4.62e-01   | 4.06e-26 | NA        | NA          | NA        |

711  
712

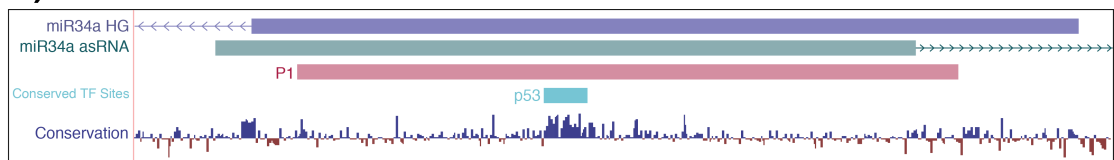
713 **Figure 1 Supplement 1:** A) Spearman's rho and p-values (p) from the correlation analysis  
714 investigating the correlation between miR34a and miR34a asRNA expression in TP53 wild type (wt)  
715 and mutated (mut) samples within TCGA cancer types. Bladder Urothelial Carcinoma (BLCA), Breast  
716 invasive carcinoma (BRCA), Head and Neck squamous cell carcinoma (HNSC), Lower Grade Glioma  
717 (LGG), Liver hepatocellular carcinoma (LIHC), Lung adenocarcinoma (LUAD), Lung squamous cell  
718 carcinoma (LUSC), Ovarian serous cystadenocarcinoma (OV), Prostate adenocarcinoma (PRAD), Skin  
719 Cutaneous Melanoma (SKCM), Stomach adenocarcinoma (STAD).



720  
721  
722  
723  
724  
725  
726  
727  
728  
729  
730  
731

**Figure 1 Supplement 2:** **A)** A schematic representation of the primer placement in the primer walk assay. **B)** Polyadenylation status of spliced and unspliced miR34a asRNA in HEK293T cells. **C)** Sequencing results from the analysis of *miR34a* asRNA isoforms in U2OS cells. *miR34a* AS ref. refers to the full length transcript as defined by the 3'-RACE and primer walk assay. **D)** Analysis of coding potential of the *miR34a* asRNA transcript using the Coding-potential Calculator. **E)** RNAseq data from five fractionated cell lines in the ENCODE project showing the percentage of transcripts per million (TPM) for miR34a asRNA. MALAT1 (nuclear localization) and GAPDH (cytoplasmic localization) are included as fractionation controls. Points represent the mean and horizontal lines represent the standard deviation from two biological replicates.

**A)**

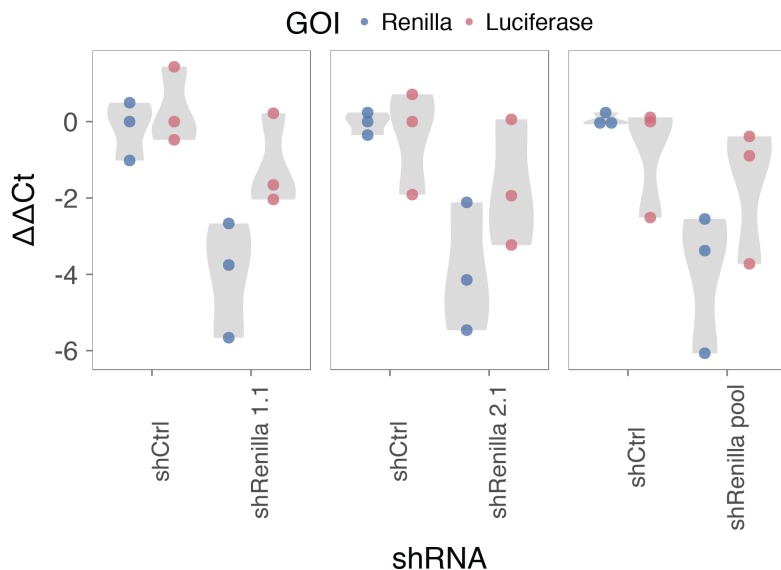


**B)**



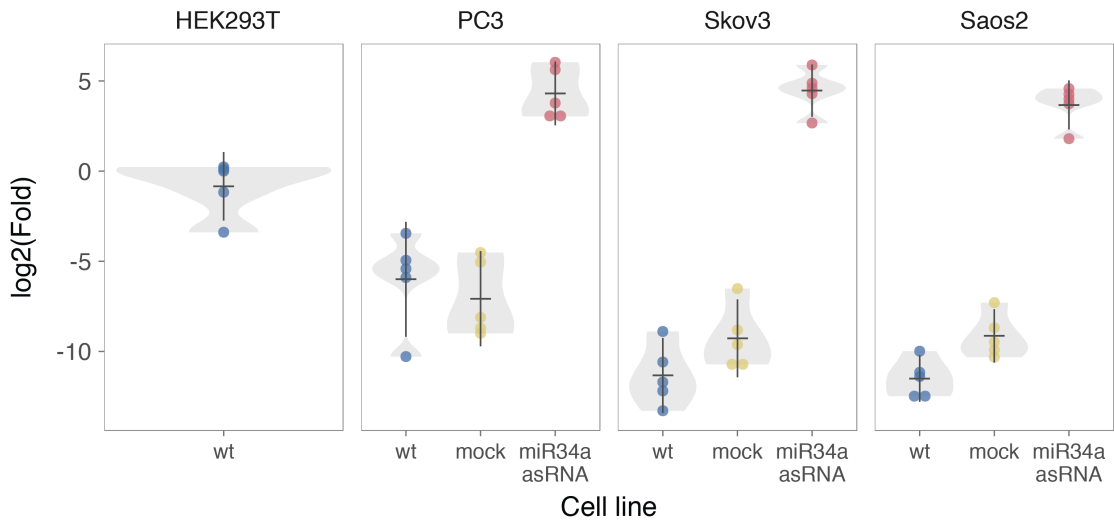
732  
733  
734  
735  
736  
737

**Figure 2 Supplement 1:** **A)** A UCSC genome browser illustration indicating the location of the promoter region cloned into the p1 construct including the conserved TP53-binding site. **B)** A representative picture of the p1 construct including forward (F) and reverse (R) primer locations and the renilla shRNA targeting site.



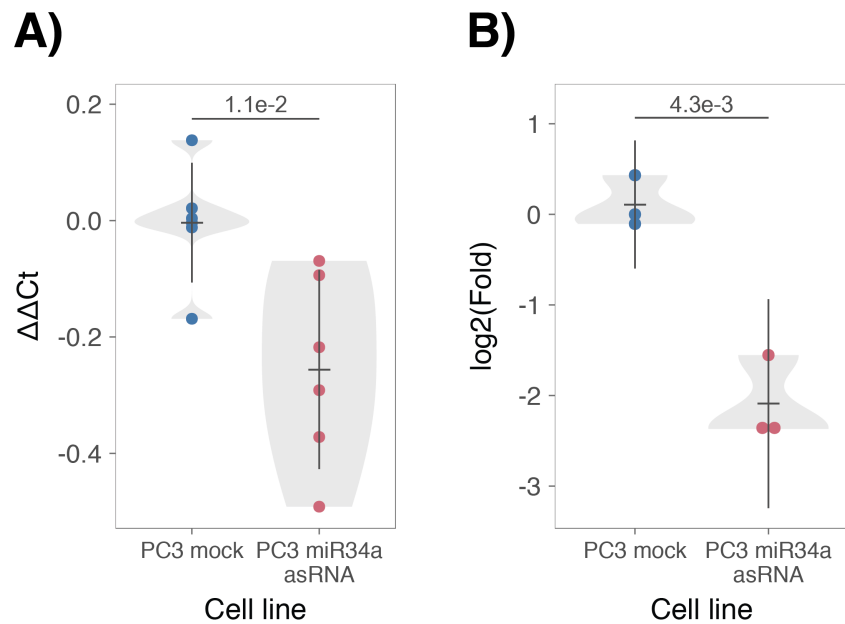
738  
739  
740  
741  
742  
743

**Figure 2 Supplement 2:** HEK293T cells were co-transfected with the P1 construct and either shRenilla or shControl. Renilla and luciferase levels were measured with Q-PCR 48 hours after transfection. Individual points represent independent experiments with the gray shadow indicating the density of the points.



744  
745  
746  
747  
748

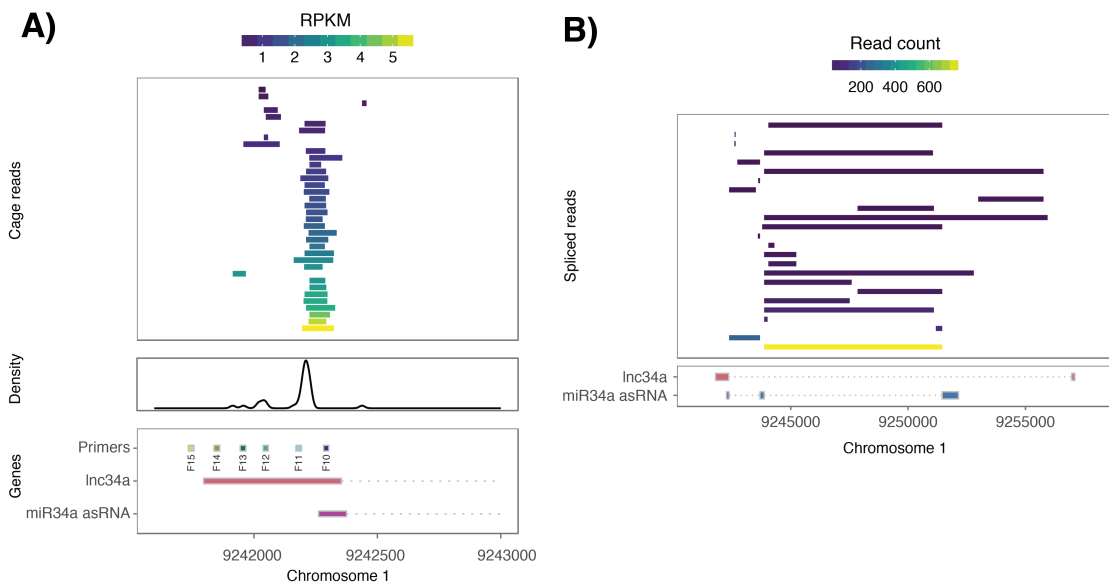
**Figure 3 Supplement 1:** Comparison of *miR34a* asRNA expression in HEK293T cells (high endogenous *miR34a* asRNA), and the wild-type (wt), mock, and *miR34a* over-expressing stable cell lines.



749  
750  
751  
752

**Figure 3 Supplement 2:** CCND1 expression (A) and western blot quantification of protein levels (B) in *miR34a* asRNA over-expressing PC3 stable cell lines.

753  
754  
755  
756  
757  
758  
759  
760  
761  
762



**Supplementary Figure 4:** A) CAGE transcription start sites from 28 ENCODE cell lines which mapped between 200 base pairs upstream of the *lnc34a* start site and 200 base pairs upstream of the GENCODE annotated *miR34a* asRNA start site (top panel). The density of the CAGE reads (middle panel) and the transcription start regions for *lnc34a* and the annotated *miR34a* asRNA, as well as, primer positions from the primer walk assay (bottom panel) are also illustrated. B) Spliced reads from 36 ENCODE cell lines which had reads mapping to the *lnc34a/miR34a* asRNA locus (top panel) and the *lnc34a* and *miR34a* asRNA genes (bottom panel).

763

764 **References**

765

766 Agostini, M., P. Tucci, R. Killick, E. Candi, B. S. Sayan, P. Rivetti di Val Cervo, P.  
 767 Nicotera, F. McKeon, R. A. Knight, T. W. Mak and G. Melino (2011). "Neuronal  
 768 differentiation by TAp73 is mediated by microRNA-34a regulation of synaptic  
 769 protein targets." *Proc Natl Acad Sci U S A* **108**(52): 21093-21098. DOI:  
 770 10.1073/pnas.1112061109

771

772 Ahn, Y. H., D. L. Gibbons, D. Chakravarti, C. J. Creighton, Z. H. Rizvi, H. P. Adams, A.  
 773 Pertsemlidis, P. A. Gregory, J. A. Wright, G. J. Goodall, E. R. Flores and J. M. Kurie  
 774 (2012). "ZEB1 drives prometastatic actin cytoskeletal remodeling by  
 775 downregulating miR-34a expression." *J Clin Invest* **122**(9): 3170-3183. DOI:  
 776 10.1172/JCI63608

777

778 Allaire, J., Y. Xie, J. McPherson, J. Luraschi, K. Ushey, A. Atkins, H. Wickham, J.  
 779 Cheng and W. Chang (2017). rmarkdown: Dynamic Documents for R. R package  
 780 version 1.8. <https://CRAN.R-project.org/package=rmarkdown>

781

782 Amarzguioui, M., J. J. Rossi and D. Kim (2005). "Approaches for chemically  
 783 synthesized siRNA and vector-mediated RNAi." *FEBS Lett* **579**(26): 5974-5981.  
 784 DOI: 10.1016/j.febslet.2005.08.070

785

786 Arnold, J. B. (2017). ggthemes: Extra Themes, Scales and Geoms for 'ggplot2'. R  
 787 package version 3.4.0. <https://CRAN.R-project.org/package=ggthemes>

788

789 Ashouri, A., V. I. Sayin, J. Van den Eynden, S. X. Singh, T. Papagiannakopoulos and  
 790 E. Larsson (2016). "Pan-cancer transcriptomic analysis associates long non-  
 791 coding RNAs with key mutational driver events." *Nature Communications* **7**:  
 792 13197. DOI: 10.1038/ncomms13197

793

794 Balbin, O. A., R. Malik, S. M. Dhanasekaran, J. R. Prensner, X. Cao, Y. M. Wu, D.  
 795 Robinson, R. Wang, G. Chen, D. G. Beer, A. I. Nesvizhskii and A. M. Chinnaian  
 796 (2015). "The landscape of antisense gene expression in human cancers." *Genome  
 797 Res* **25**(7): 1068-1079. DOI: 10.1101/gr.180596.114

798

799 Boque-Sastre, R., M. Soler, C. Oliveira-Mateos, A. Portela, C. Moutinho, S. Sayols, A.  
 800 Villanueva, M. Esteller and S. Guil (2015). "Head-to-head antisense transcription  
 801 and R-loop formation promotes transcriptional activation." *Proc Natl Acad Sci U  
 802 S A* **112**(18): 5785-5790. DOI: 10.1073/pnas.1421197112

803

804 Chang, T. C., D. Yu, Y. S. Lee, E. A. Wentzel, D. E. Arking, K. M. West, C. V. Dang, A.  
 805 Thomas-Tikhonenko and J. T. Mendell (2008). "Widespread microRNA  
 806 repression by Myc contributes to tumorigenesis." *Nat Genet* **40**(1): 43-50. DOI:  
 807 10.1038/ng.2007.30

808

809 Chang, W. (2014). extrafont: Tools for using fonts. R package version 0.17.  
 810 <https://CRAN.R-project.org/package=extrafont>

811

- 812 Chen, J., M. Sun, W. J. Kent, X. Huang, H. Xie, W. Wang, G. Zhou, R. Z. Shi and J. D.  
813 Rowley (2004). "Over 20% of human transcripts might form sense-antisense  
814 pairs." *Nucleic Acids Res* **32**(16): 4812-4820. DOI: 10.1093/nar/gkh818
- 815
- 816 Cheng, J., L. Zhou, Q. F. Xie, H. Y. Xie, X. Y. Wei, F. Gao, C. Y. Xing, X. Xu, L. J. Li and S.  
817 S. Zheng (2010). "The impact of miR-34a on protein output in hepatocellular  
818 carcinoma HepG2 cells." *Proteomics* **10**(8): 1557-1572. DOI:  
819 10.1002/pmic.200900646
- 820
- 821 Chim, C. S., K. Y. Wong, Y. Qi, F. Loong, W. L. Lam, L. G. Wong, D. Y. Jin, J. F. Costello  
822 and R. Liang (2010). "Epigenetic inactivation of the miR-34a in hematological  
823 malignancies." *Carcinogenesis* **31**(4): 745-750. DOI: 10.1093/carcin/bgq033
- 824
- 825 Cole, K. A., E. F. Attiyeh, Y. P. Mosse, M. J. Laquaglia, S. J. Diskin, G. M. Brodeur and  
826 J. M. Maris (2008). "A functional screen identifies miR-34a as a candidate  
827 neuroblastoma tumor suppressor gene." *Mol Cancer Res* **6**(5): 735-742. DOI:  
828 10.1158/1541-7786.MCR-07-2102
- 829
- 830 Conley, A. B. and I. K. Jordan (2012). "Epigenetic regulation of human cis-natural  
831 antisense transcripts." *Nucleic Acids Res* **40**(4): 1438-1445. DOI:  
832 10.1093/nar/gkr1010
- 833
- 834 Consortium, E. P. (2012). "An integrated encyclopedia of DNA elements in the  
835 human genome." *Nature* **489**(7414): 57-74. DOI: 10.1038/nature11247
- 836
- 837 Ding, N., H. Wu, T. Tao and E. Peng (2017). "NEAT1 regulates cell proliferation  
838 and apoptosis of ovarian cancer by miR-34a-5p/BCL2." *Onco Targets Ther* **10**:  
839 4905-4915. DOI: 10.2147/OTT.S142446
- 840
- 841 Djebali, S., C. A. Davis, A. Merkel, A. Dobin, T. Lassmann, A. Mortazavi, A. Tanzer, J.  
842 Lagarde, W. Lin, F. Schlesinger, C. Xue, G. K. Marinov, J. Khatun, B. A. Williams, C.  
843 Zaleski, J. Rozowsky, M. Roder, F. Kokocinski, R. F. Abdelhamid, T. Alioto, I.  
844 Antoshechkin, M. T. Baer, N. S. Bar, P. Batut, K. Bell, I. Bell, S. Chakrabortty, X.  
845 Chen, J. Chrast, J. Curado, T. Derrien, J. Drenkow, E. Dumais, J. Dumais, R.  
846 Duttagupta, E. Falconnet, M. Fastuca, K. Fejes-Toth, P. Ferreira, S. Foissac, M. J.  
847 Fullwood, H. Gao, D. Gonzalez, A. Gordon, H. Gunawardena, C. Howald, S. Jha, R.  
848 Johnson, P. Kapranov, B. King, C. Kingswood, O. J. Luo, E. Park, K. Persaud, J. B.  
849 Preall, P. Ribeca, B. Risk, D. Robyr, M. Sammeth, L. Schaffer, L. H. See, A. Shahab, J.  
850 Skancke, A. M. Suzuki, H. Takahashi, H. Tilgner, D. Trout, N. Walters, H. Wang, J.  
851 Wrobel, Y. Yu, X. Ruan, Y. Hayashizaki, J. Harrow, M. Gerstein, T. Hubbard, A.  
852 Reymond, S. E. Antonarakis, G. Hannon, M. C. Giddings, Y. Ruan, B. Wold, P.  
853 Carninci, R. Guigo and T. R. Gingeras (2012). "Landscape of transcription in  
854 human cells." *Nature* **489**(7414): 101-108. DOI: 10.1038/nature11233
- 855
- 856 Gallardo, E., A. Navarro, N. Vinolas, R. M. Marrades, T. Diaz, B. Gel, A. Quera, E.  
857 Bandres, J. Garcia-Foncillas, J. Ramirez and M. Monzo (2009). "miR-34a as a  
858 prognostic marker of relapse in surgically resected non-small-cell lung cancer."  
859 *Carcinogenesis* **30**(11): 1903-1909. DOI: 10.1093/carcin/bgp219
- 860

- 861 Hunten, S., M. Kaller, F. Drepper, S. Oeljeklaus, T. Bonfert, F. Erhard, A. Dueck, N.  
862 Eichner, C. C. Friedel, G. Meister, R. Zimmer, B. Warscheid and H. Hermeking  
863 (2015). "p53-Regulated Networks of Protein, mRNA, miRNA, and lncRNA  
864 Expression Revealed by Integrated Pulsed Stable Isotope Labeling With Amino  
865 Acids in Cell Culture (pSILAC) and Next Generation Sequencing (NGS) Analyses."  
866 Mol Cell Proteomics **14**(10): 2609-2629. DOI: 10.1074/mcp.M115.050237  
867
- 868 International Human Genome Sequencing, C. (2004). "Finishing the euchromatic  
869 sequence of the human genome." Nature **431**(7011): 931-945. DOI:  
870 10.1038/nature03001  
871
- 872 Johnsson, P., A. Ackley, L. Vidarsdottir, W. O. Lui, M. Corcoran, D. Grander and K.  
873 V. Morris (2013). "A pseudogene long-noncoding-RNA network regulates PTEN  
874 transcription and translation in human cells." Nat Struct Mol Biol **20**(4): 440-  
875 446. DOI: 10.1038/nsmb.2516  
876
- 877 Katayama, S., Y. Tomaru, T. Kasukawa, K. Waki, M. Nakanishi, M. Nakamura, H.  
878 Nishida, C. C. Yap, M. Suzuki, J. Kawai, H. Suzuki, P. Carninci, Y. Hayashizaki, C.  
879 Wells, M. Frith, T. Ravasi, K. C. Pang, J. Hallinan, J. Mattick, D. A. Hume, L. Lipovich,  
880 S. Batalov, P. G. Engstrom, Y. Mizuno, M. A. Faghihi, A. Sandelin, A. M. Chalk, S.  
881 Mottagui-Tabar, Z. Liang, B. Lenhard, C. Wahlestedt, R. G. E. R. Group, G. Genome  
882 Science and F. Consortium (2005). "Antisense transcription in the mammalian  
883 transcriptome." Science **309**(5740): 1564-1566. DOI: 10.1126/science.1112009  
884
- 885 Kent, W. J., C. W. Sugnet, T. S. Furey, K. M. Roskin, T. H. Pringle, A. M. Zahler and D.  
886 Haussler (2002). "The human genome browser at UCSC." Genome Res **12**(6):  
887 996-1006. DOI: 10.1101/gr.229102. Article published online before print in May  
888 2002  
889
- 890 Kim, K. H., H. J. Kim and T. R. Lee (2017). "Epidermal long non-coding RNAs are  
891 regulated by ultraviolet irradiation." Gene **637**: 196-202. DOI:  
892 10.1016/j.gene.2017.09.043  
893
- 894 Kong, L., Y. Zhang, Z. Q. Ye, X. Q. Liu, S. Q. Zhao, L. Wei and G. Gao (2007). "CPC:  
895 assess the protein-coding potential of transcripts using sequence features and  
896 support vector machine." Nucleic Acids Res **35**(Web Server issue): W345-349.  
897 DOI: 10.1093/nar/gkm391  
898
- 899 Lal, A., M. P. Thomas, G. Altschuler, F. Navarro, E. O'Day, X. L. Li, C. Concepcion, Y.  
900 C. Han, J. Thiery, D. K. Rajani, A. Deutsch, O. Hofmann, A. Ventura, W. Hide and J.  
901 Lieberman (2011). "Capture of microRNA-bound mRNAs identifies the tumor  
902 suppressor miR-34a as a regulator of growth factor signaling." PLoS Genet **7**(11):  
903 e1002363. DOI: 10.1371/journal.pgen.1002363  
904
- 905 Leveille, N., C. A. Melo, K. Rooijers, A. Diaz-Lagares, S. A. Melo, G. Korkmaz, R.  
906 Lopes, F. Akbari Moqadam, A. R. Maia, P. J. Wijchers, G. Geeven, M. L. den Boer, R.  
907 Kalluri, W. de Laat, M. Esteller and R. Agami (2015). "Genome-wide profiling of  
908 p53-regulated enhancer RNAs uncovers a subset of enhancers controlled by a  
909 lncRNA." Nature Communications **6**: 6520. DOI: 10.1038/ncomms7520

- 910  
911 Liu, C., K. Kelnar, B. Liu, X. Chen, T. Calhoun-Davis, H. Li, L. Patrawala, H. Yan, C.  
912 Jeter, S. Honorio, J. F. Wiggins, A. G. Bader, R. Fagin, D. Brown and D. G. Tang  
913 (2011). "The microRNA miR-34a inhibits prostate cancer stem cells and  
914 metastasis by directly repressing CD44." *Nat Med* **17**(2): 211-215. DOI:  
915 10.1038/nm.2284
- 916  
917 Memczak, S., M. Jens, A. Elefsinioti, F. Torti, J. Krueger, A. Rybak, L. Maier, S. D.  
918 Mackowiak, L. H. Gregersen, M. Munschauer, A. Loewer, U. Ziebold, M.  
919 Landthaler, C. Kocks, F. le Noble and N. Rajewsky (2013). "Circular RNAs are a  
920 large class of animal RNAs with regulatory potency." *Nature* **495**(7441): 333-  
921 338. DOI: 10.1038/nature11928
- 922  
923 O'Leary, N. A., M. W. Wright, J. R. Brister, S. Ciufo, D. Haddad, R. McVeigh, B.  
924 Rajput, B. Robbertse, B. Smith-White, D. Ako-Adjei, A. Astashyn, A. Badretdin, Y.  
925 Bao, O. Blinkova, V. Brover, V. Chetvernin, J. Choi, E. Cox, O. Ermolaeva, C. M.  
926 Farrell, T. Goldfarb, T. Gupta, D. Haft, E. Hatcher, W. Hlavina, V. S. Joardar, V. K.  
927 Kodali, W. Li, D. Maglott, P. Masterson, K. M. McGarvey, M. R. Murphy, K. O'Neill,  
928 S. Pujar, S. H. Rangwala, D. Rausch, L. D. Riddick, C. Schoch, A. Shkeda, S. S. Storz,  
929 H. Sun, F. Thibaud-Nissen, I. Tolstoy, R. E. Tully, A. R. Vatsan, C. Wallin, D. Webb,  
930 W. Wu, M. J. Landrum, A. Kimchi, T. Tatusova, M. DiCuccio, P. Kitts, T. D. Murphy  
931 and K. D. Pruitt (2016). "Reference sequence (RefSeq) database at NCBI: current  
932 status, taxonomic expansion, and functional annotation." *Nucleic Acids Res*  
933 **44**(D1): D733-745. DOI: 10.1093/nar/gkv1189
- 934  
935 Ozsolak, F., P. Kapranov, S. Foissac, S. W. Kim, E. Fishilevich, A. P. Monaghan, B.  
936 John and P. M. Milos (2010). "Comprehensive polyadenylation site maps in yeast  
937 and human reveal pervasive alternative polyadenylation." *Cell* **143**(6): 1018-  
938 1029. DOI: 10.1016/j.cell.2010.11.020
- 939  
940 Polson, A., E. Durrett and D. Reisman (2011). "A bidirectional promoter reporter  
941 vector for the analysis of the p53/WDR79 dual regulatory element." *Plasmid*  
942 **66**(3): 169-179. DOI: 10.1016/j.plasmid.2011.08.004
- 943  
944 Rashi-Elkeles, S., H. J. Warnatz, R. Elkon, A. Kupershtein, Y. Chobod, A. Paz, V.  
945 Amstislavskiy, M. Sultan, H. Safer, W. Nietfeld, H. Lehrach, R. Shamir, M. L. Yaspo  
946 and Y. Shiloh (2014). "Parallel profiling of the transcriptome, cistrome, and  
947 epigenome in the cellular response to ionizing radiation." *Sci Signal* **7**(325): rs3.  
948 DOI: 10.1126/scisignal.2005032
- 949  
950 Raver-Shapira, N., E. Marciano, E. Meiri, Y. Spector, N. Rosenfeld, N. Moskovits, Z.  
951 Bentwich and M. Oren (2007). "Transcriptional activation of miR-34a  
952 contributes to p53-mediated apoptosis." *Mol Cell* **26**(5): 731-743. DOI:  
953 10.1016/j.molcel.2007.05.017
- 954  
955 Rinn, J. L., M. Kertesz, J. K. Wang, S. L. Squazzo, X. Xu, S. A. Brugmann, L. H.  
956 Goodnough, J. A. Helms, P. J. Farnham, E. Segal and H. Y. Chang (2007).  
957 "Functional demarcation of active and silent chromatin domains in human HOX

958 loci by noncoding RNAs." *Cell* **129**(7): 1311-1323. DOI:  
959 10.1016/j.cell.2007.05.022  
960  
961 Rokavec, M., M. G. Oner, H. Li, R. Jackstadt, L. Jiang, D. Lodygin, M. Kaller, D. Horst,  
962 P. K. Ziegler, S. Schwitalla, J. Slotta-Huspenina, F. G. Bader, F. R. Greten and H.  
963 Hermeking (2015). "Corrigendum. IL-6R/STAT3/miR-34a feedback loop  
964 promotes EMT-mediated colorectal cancer invasion and metastasis." *J Clin Invest*  
965 **125**(3): 1362. DOI: 10.1172/JCI81340  
966  
967 Schneider, C. A., W. S. Rasband and K. W. Eliceiri (2012). "NIH Image to ImageJ:  
968 25 years of image analysis." *Nat Methods* **9**(7): 671-675.  
969  
970 Serviss, J. T. (2017). miR34AasRNaproject.  
971 [https://github.com/GranderLab/miR34a\\_asRNA\\_project](https://github.com/GranderLab/miR34a_asRNA_project)  
972  
973 Serviss, J. T., P. Johnsson and D. Grander (2014). "An emerging role for long non-  
974 coding RNAs in cancer metastasis." *Front Genet* **5**: 234. DOI:  
975 10.3389/fgene.2014.00234  
976  
977 Slabakova, E., Z. Culig, J. Remsik and K. Soucek (2017). "Alternative mechanisms  
978 of miR-34a regulation in cancer." *Cell Death Dis* **8**(10): e3100. DOI:  
979 10.1038/cddis.2017.495  
980  
981 Stahlhut, C. and F. J. Slack (2015). "Combinatorial Action of MicroRNAs let-7 and  
982 miR-34 Effectively Synergizes with Erlotinib to Suppress Non-small Cell Lung  
983 Cancer Cell Proliferation." *Cell Cycle* **14**(13): 2171-2180. DOI:  
984 10.1080/15384101.2014.1003008  
985  
986 Su, X., D. Chakravarti, M. S. Cho, L. Liu, Y. J. Gi, Y. L. Lin, M. L. Leung, A. El-Naggar,  
987 C. J. Creighton, M. B. Suraokar, I. Wistuba and E. R. Flores (2010). "TAp63  
988 suppresses metastasis through coordinate regulation of Dicer and miRNAs."  
989 *Nature* **467**(7318): 986-990. DOI: 10.1038/nature09459  
990  
991 Sun, F., H. Fu, Q. Liu, Y. Tie, J. Zhu, R. Xing, Z. Sun and X. Zheng (2008).  
992 "Downregulation of CCND1 and CDK6 by miR-34a induces cell cycle arrest."  
993 *FEBS Lett* **582**(10): 1564-1568. DOI: 10.1016/j.febslet.2008.03.057  
994  
995 Team, R. C. (2017). "R: A Language and Environment for Statistical Computing."  
996 from <https://www.R-project.org/>.  
997  
998 Turner, A. M., A. M. Ackley, M. A. Matrone and K. V. Morris (2012).  
999 "Characterization of an HIV-targeted transcriptional gene-silencing RNA in  
1000 primary cells." *Hum Gene Ther* **23**(5): 473-483. DOI: 10.1089/hum.2011.165  
1001  
1002 Vogt, M., J. Mundig, M. Gruner, S. T. Liffers, B. Verdoodt, J. Hauk, L.  
1003 Steinstraesser, A. Tannapfel and H. Hermeking (2011). "Frequent concomitant  
1004 inactivation of miR-34a and miR-34b/c by CpG methylation in colorectal,  
1005 pancreatic, mammary, ovarian, urothelial, and renal cell carcinomas and soft

1006 tissue sarcomas." *Virchows Arch* **458**(3): 313-322. DOI: 10.1007/s00428-010-  
1007 1030-5  
1008  
1009 Wang, L., P. Bu, Y. Ai, T. Srinivasan, H. J. Chen, K. Xiang, S. M. Lipkin and X. Shen  
1010 (2016). "A long non-coding RNA targets microRNA miR-34a to regulate colon  
1011 cancer stem cell asymmetric division." *eLife* **5**. DOI: 10.7554/eLife.14620  
1012  
1013 Wang, L., H. J. Park, S. Dasari, S. Wang, J. P. Kocher and W. Li (2013). "CPAT:  
1014 Coding-Potential Assessment Tool using an alignment-free logistic regression  
1015 model." *Nucleic Acids Res* **41**(6): e74. DOI: 10.1093/nar/gkt006  
1016  
1017 Wang, X., J. Li, K. Dong, F. Lin, M. Long, Y. Ouyang, J. Wei, X. Chen, Y. Weng, T. He  
1018 and H. Zhang (2015). "Tumor suppressor miR-34a targets PD-L1 and functions  
1019 as a potential immunotherapeutic target in acute myeloid leukemia." *Cell Signal*  
1020 **27**(3): 443-452. DOI: 10.1016/j.cellsig.2014.12.003  
1021  
1022 Wickham, H. (2016). gtable: Arrange 'Grobs' in Tables. R package version 0.2.0.  
1023 <https://CRAN.R-project.org/package=gtable>  
1024  
1025 Wickham, H. (2017). scales: Scale Functions for Visualization. R package version  
1026 0.5.0. <https://CRAN.R-project.org/package=scales>  
1027  
1028 Wickham, H. (2017). tidyverse: Easily Install and Load the 'Tidyverse'. R package  
1029 version 1.2.1. <https://CRAN.R-project.org/package=tidyverse>  
1030  
1031 Wickham, L. H. a. H. (2017). rlang: Functions for Base Types and Core R and  
1032 'Tidyverse' Features. R package version 0.1.4. [https://CRAN.R-  
1033 project.org/package=rlang](https://CRAN.R-project.org/package=rlang)  
1034  
1035 Wickham, S. M. B. a. H. (2014). magrittr: A Forward-Pipe Operator for R. R  
1036 package version 1.5. <https://CRAN.R-project.org/package=magrittr>  
1037  
1038 Wilkins, D. ggenes: Draw Gene Arrow Maps in 'ggplot2'. R package version  
1039 0.2.0.9003. <https://github.com/wilkox/ggenes>  
1040  
1041 Xiao, N. (2017). liftr: Containerize R Markdown Documents. R package version  
1042 0.7. <https://CRAN.R-project.org/package=liftr>  
1043  
1044 Xie, Y. (2017). knitr: A General-Purpose Package for Dynamic Report Generation  
1045 in R. R package version 1.17. <https://yihui.name/knitr/>  
1046  
1047 Yang, P., Q. J. Li, Y. Feng, Y. Zhang, G. J. Markowitz, S. Ning, Y. Deng, J. Zhao, S.  
1048 Jiang, Y. Yuan, H. Y. Wang, S. Q. Cheng, D. Xie and X. F. Wang (2012). "TGF-beta-  
1049 miR-34a-CCL22 signaling-induced Treg cell recruitment promotes venous  
1050 metastases of HBV-positive hepatocellular carcinoma." *Cancer Cell* **22**(3): 291-  
1051 303. DOI: 10.1016/j.ccr.2012.07.023  
1052  
1053 Yap, K. L., S. Li, A. M. Munoz-Cabello, S. Raguz, L. Zeng, S. Mujtaba, J. Gil, M. J.  
1054 Walsh and M. M. Zhou (2010). "Molecular interplay of the noncoding RNA ANRIL

1055 and methylated histone H3 lysine 27 by polycomb CBX7 in transcriptional  
1056 silencing of INK4a." Mol Cell **38**(5): 662-674. DOI: 10.1016/j.molcel.2010.03.021  
1057  
1058 Yu, W., D. Gius, P. Onyango, K. Muldoon-Jacobs, J. Karp, A. P. Feinberg and H. Cui  
1059 (2008). "Epigenetic silencing of tumour suppressor gene p15 by its antisense  
1060 RNA." Nature **451**(7175): 202-206. DOI: 10.1038/nature06468  
1061  
1062 Zenz, T., J. Mohr, E. Eldering, A. P. Kater, A. Buhler, D. Kienle, D. Winkler, J. Durig,  
1063 M. H. van Oers, D. Mertens, H. Dohner and S. Stilgenbauer (2009). "miR-34a as  
1064 part of the resistance network in chronic lymphocytic leukemia." Blood **113**(16):  
1065 3801-3808. DOI: 10.1182/blood-2008-08-172254  
1066  
1067